optotune
shaping the future of optics

TU Delft
Delft University of Technology

Department of Precision and Microsystems Engineering

Tunable Optofluidic Aperture

Name: J.T.M. Mutsaerts

Report no: ME 10.041
Coach: Ir. J. Spronck, Dr.ir. J.F.L. Goosen, Dr. C. Graetzel
Professor: Prof ir. R.H. Munnig Schmidt
Specialisation: Mechatronic System Design
Type of report: Thesis Master of Science
Date: 03-02-2011

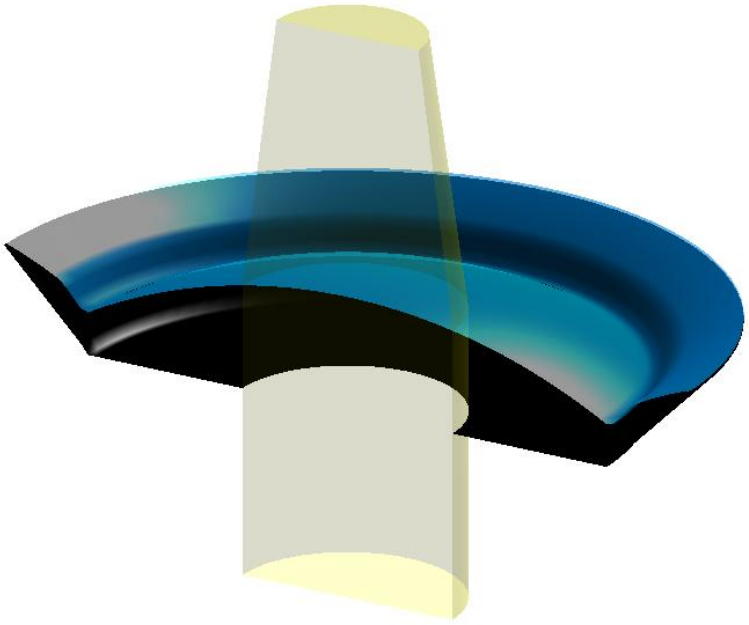

Preface

This thesis report represents the final work for an intensive Master thesis period of eight months at Optotune in Zürich. At the same time, this report represents the final work for my studies Mechatronic System Design at the Delft University of Technology.

I would like to thank my supervisors in Delft: Jo Spronck, Hans Goosen and Rob Munnig Schmidt for trusting me to write my thesis research in Zürich and for their continuous support.

My thanks also go to the great people at Optotune, for providing me with challenging subjects, support and a fair portion of startup atmosphere. Special thanks go to Chauncey Graetzel, my supervisor at Optotune, who was always there to provide me with objective feedback and smart insights. His dedication to coaching me brought him even twice to Delft, which I could not have expected.

Finally, I thank my family and friends for their support over the whole seven years of studies. Thank you all!

Joep Mutsaerts

Zürich, February 2011

1 Abstract

Optotune AG, based in Zürich, Switzerland, produces tunable lenses by using a hydrostatic pressure in combination with a viscoelastic silicone membrane. In this thesis, the lens technique is used to develop a tunable aperture. Furthermore, the influence of membrane design parameters on the required actuation force has been investigated.

Tunable Optofluidic Aperture

Conventional tunable lens designs comprise a transparent fluid contained by a glass plate and a silicone membrane in axisymmetric setup. The use of a light absorbing fluid instead of a transparent fluid creates a tunable aperture. Application of such apertures can be advantageous in the mobile camera phone market because of their small size and cheap production.
The concept of the aperture was proven by building demonstrators. Two architectures have been used, a single and double liquid design. Both designs repeatedly showed trapped fluid in the center of the aperture, which is an undesired effect.
Experiments were done to investigate the influence of several parameters on the dark spot in the center. Surface tension, contact angle, hydrophilic properties, glass coating, particle size , particle concentration, pressure and fluid viscosity were tested. Only pigment particle size and concentration showed a large influence on the dark spot. If the concentration of particles is low enough and the size of particles is small enough, a clear aperture is created. However, the clear aperture showed a soft aperture edge. This soft edge caused a lens effect.
The lens effect can be compensated for in a double liquid design with one dark and one transparent fluid having matching refractive indexes. While prototyping, the pigments diffused through the membrane to the transparent fluid, which colored the transparent fluid red. Furthermore, the double liquid design is more complicated to mass produce in mobile phone size.

Membrane model identification

Any tunable lens or aperture containing a silicone membrane and fluid container needs an actuation force (hydrostatic pressure) to reach a focal length (lens deflection). The required pressure depends on the design parameters of the silicone membrane. This thesis enables Optotune to estimate the needed pressure, while varying design parameters. A correct estimation of the required pressure and actuation force will save development time of Optotune's products.
The deflection versus pressure relation of Optotune's silicone membranes is investigated in this thesis. The shape of the membrane is modeled as a spherical cap. Various aperture diameters, thicknesses, prestrains and deflections have been measured. The stress strain curves of the membranes were fitted with a Mooney Rivlin material model. A developed 'Shape Predictor' software uses this model to instantly model a lens shape and can calculate several properties such as the force needed to drive the lens.

Conclusion
This thesis proved the functionality of the tunable optofluidic aperture but could not eliminate certain side effects. Research results on the material model has created a better understanding of the membrane material. Software tools have been developed to be use the research in production and design at Optotune.

Index

2 List of variables

λ	[-]	Material stretch: ratio between new length and old length
ε	[-]	Material strain: ratio between extension and old length
V	[m^3]	Volume
A	[m^2]	Area
t	[m]	Thickness
l	[m]	Length
r	[m]	Aperture / flat radius of circular membrane
R	[m]	Bulge radius
z	[m]	Deflection height of membrane bulge at center
θ	[deg]	Deflection Angle (see Fig. 37)
F	[N]	Force
σ	[Pa]	Stress
$c10, c01$	[Pa]	Mooney Rivlin parameters
Y	[Pa]	Young's modulus
α	[-]	Biaxial correction factor

3 Tunable optofluidic aperture

3.1 Why a tunable aperture ?

An aperture (Fig. 1) is used to control two photographical aspects:

- amount of light captured
- depth of field

When the aperture is wide open, more light is captured by the photo sensor. An extra effect is a very short depth of field . The photographical effect can be seen in Fig. 2. When the aperture is closed, less light is captured and a wider depth of field is obtained (Fig. 3).

Fig. 1 Aperture mechanism of Canon 50mm f/1.8 II lens

Fig. 2 At f/5.6, the flowers are isolated from the background.

Fig. 3 At *f*/32, the background competes for the viewer's attention.

3.2 Design motivation for tunable aperture

Current mobile phone lenses do not use an adjustable aperture yet. In the trend of increasing the photographic quality of mobile phone cameras, the adjustable aperture could play an important role. The aperture technique developed at Optotune has two main advantages.

- The aperture can be constructed small enough to fit in a mobile phone camera (< 7x7 mm)
- The aperture design potentially has a low piece count

3.3 The single liquid aperture technology

Optotune has developed tunable lenses, based on a silicone membrane containing an optical fluid. Their manually tunable lens is shown on the right. The lens is built up by an optical fluid, sandwiched between a glass plate and a silicone membrane. By turning the outer ring, the focal length can be changed.

Fig. 4 Manual Lens product

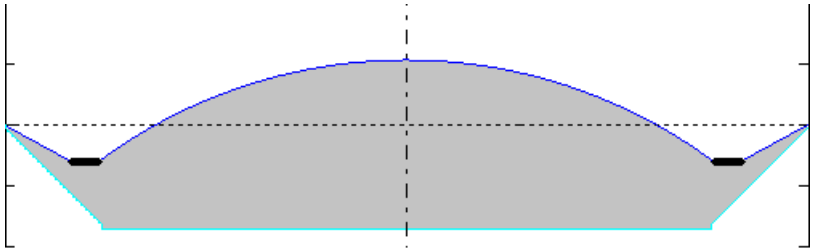

Fig. 5 cross section of the single liquid lens. A container (lightblue) containg a transparent optical liquid (grey) is closed by a membrane (dark blue). An actuator (black) pushes the sides of the membrane down. Because of constant fluid volume, the center of the membrane bulges upwards.

When the outside of the membrane is pressed down, the inside of the membrane will come up, due to the constant liquid volume. One can imagine this setup works as a convex lens When light rays are aligned with the axis of rotation. Optotune has developed this principle in a manual tunable and electrical coil tunable form. The latter has been scaled into mobile phone size, to create a zoom lens for mobile phone cameras.

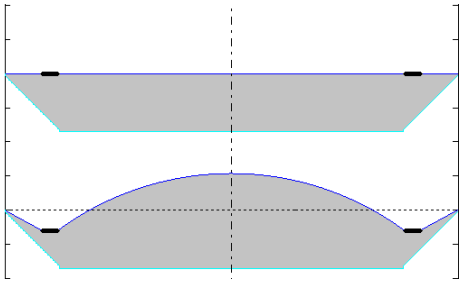

Fig. 6 flat and convex lens

Optotune discovered that when the membrane is pulled up, the inner part of the membrane touches the glass. Then a flat circle was formed on the bottom, without lens action. The circle can be enlarged by pulling up the outside of the membrane even further. The idea came that when the fluid would be dark, an aperture could be made.

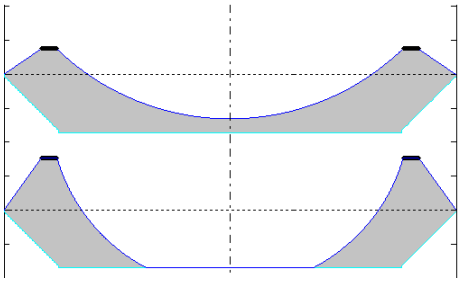

Fig. 7 concave lens and aperture

3.4 Proof of concept by the University of Singapore

Fig. 8 Aperture demonstrator by Yu Hongbin, National University of Singapore, 2008

Fig. 8 shows an optofluidic aperture, using the same principle as described in the previous section. This picture has been made during research at the National University of Singapore(Hongbin, 2008). The biggest difference with Optotune's idea is the actuation principle (here fluid is being added and removed). Furthermore, the fluid used in this demonstrator is water based. Internal experience with water based fluids used in membrane containers always showed evaporation. The water vapor simply escapes through the membranes used by Optotune (this property of membranes is used on purpose in Gore-Tex® materials).

3.5 State of the art

This section contains a brief overview of current trends in small aperture design. More information about each design can be found by searching for the patent or the given source.

Samsung roll up blades (WO 20090142050)

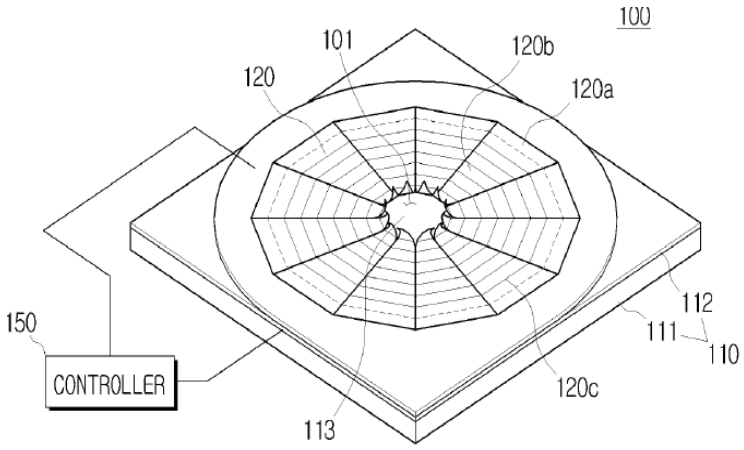

Fig. 9 Samsung Roll up blades aperture

Advantages: continuous enlargement of aperture area, fairly circular, MEMS production, clear aperture region.
Disadvantage: not yet on the market

Fribourg University – Dynamic micro iris

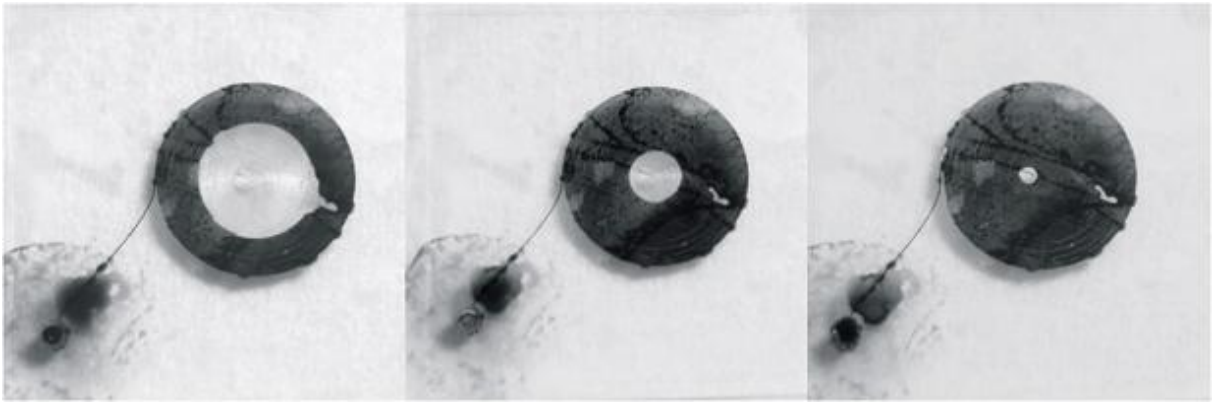

Fig. 10 Fribourg University, Dynamic microfluidic spiral iris (Müller, 2010)

Advantages: circular
Disadvantages: spiral infrastructure blocks a percentage of light, external pump/reservoir needed.

Artificial Muscle - 5 blades design

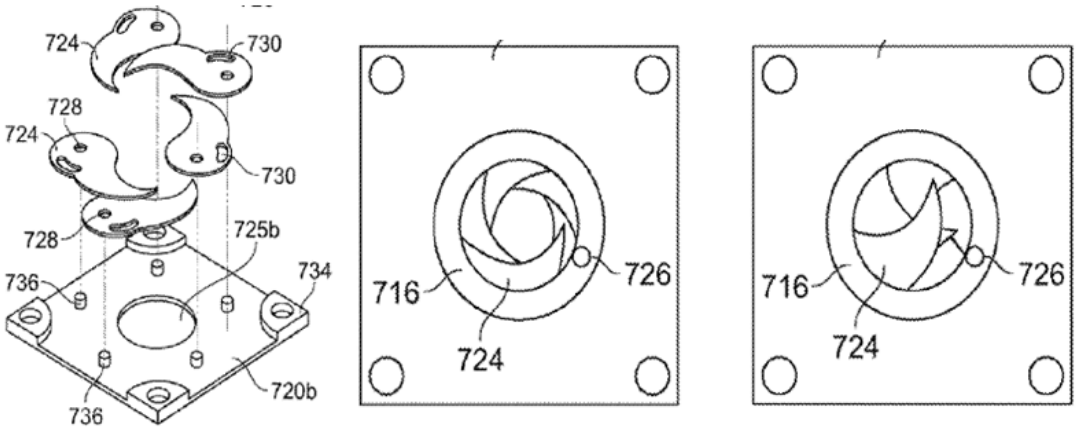

Fig. 11 Artificial Muscle, 5 blades aperture design

Advantages: clear aperture region
Disadvantage: not completely circular, many parts used

Transparent Crystals (US2008317459 A1)

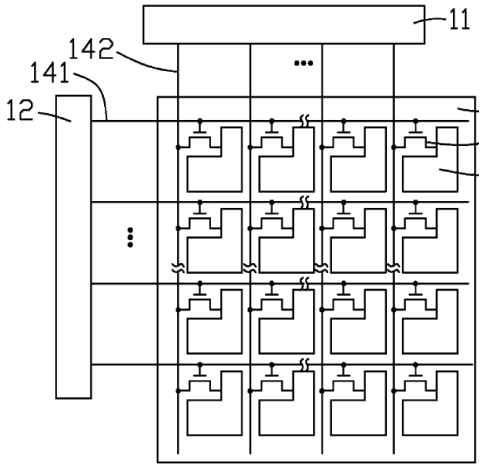

[0026] In sum, the present electrical aperture and shutter device **10** makes use of a transparence switching element **106**, e.g., a liquid crystal panel, by way of a control of an external electric field, the transparence switching element **106** would produce variations of transparence. Based upon the variations of transparence, an exposure time and an amount of passed light can be controlled and thereby the functions of aperture and shutter are achieved.

Fig. 12 Transparent Crystals, Liquid Crystal panel aperture design

Advantage: known and cheap production method
Disadvantage: low contrast

Flextronics – 2 blades (WO 2008137057)

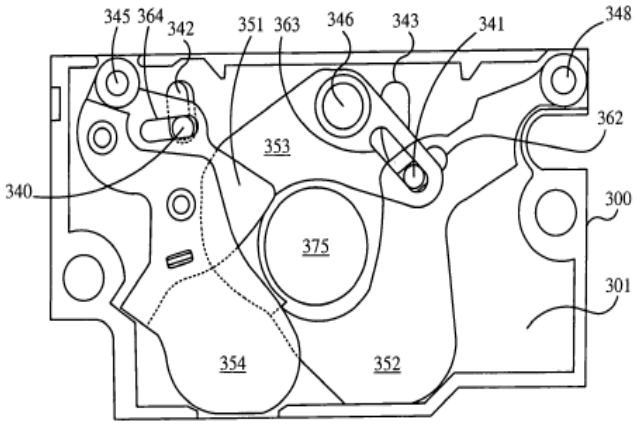

Fig. 13 Flextronics, two blades aperture design

Advantages: clear aperture region
Disadvantage: not completely circular, mechanical complexity

3.6 Technical specifications

Specifications have been made to indicate what the properties of the final product should be. This is a first indication and can be used during design of an eventual prototype. The minimal aperture is set to 0 mm, because the aperture could be used as shutter and aperture at the same time.

Optical Characteristics	
Minimum aperture diameter	0 mm
Maximum aperture diameter	2 mm
Shutter/Aperture speed	10 ms (millisecond)

Mechanical Characteristics	
Dimensions (W x H x L)	7.5 x 7.5 x 1 mm^3
Clear Aperture	2 mm
Weight	Light

Electrical Characteristics	
Power Consumption	< 50 mW
Input Voltage	2.7 V
Input Current	<20 mA
Interface to Control Electronics	I2C or PWM
Cycle Life	> 100‘000

Thermal Characteristics	
Operating Temperature	-20°C to +65°C
Storage Temperature	-40°C to + 85°C

3.7 Membrane material

This research will not discuss the membrane material, for finding the right material to use for the lenses is a huge research project on its own. Optotune is continuously performing this research in a separate department.

The membrane material used in this thesis and most of Optotune's products is internally called SE0904.

3.8 Actuation methods

This section shows various actuation methods which have been identified as suitable.

3.8.1 Electrostatic: zip actuator

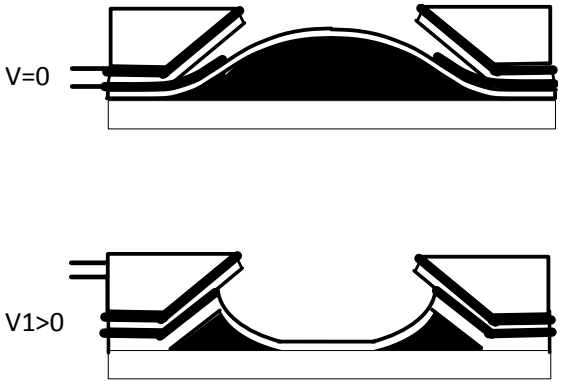

Fig. 14 Zip actuator aperture design

Electrodes are printed on the membrane. A very thin isolation layer is printed on the metal housing. A voltage difference is applied between the housing and the electrode on the membrane. Therefore the electrode is attracted to move to the housing, which changes the membrane shape.

3.8.2 Electromagnetic: ferrofluid actuator

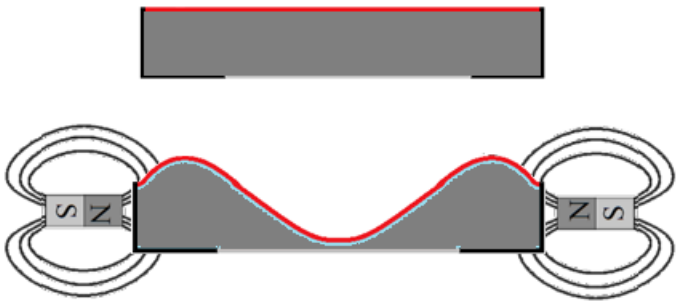

Fig. 15 Ferrofluid actuated aperture design

If ferrofluid is used as a dark fluid in the aperture, the fluid can be part of the actuator. By changing the magnetic field density at the outer diameter of the aperture setup, the fluid will be attracted to the outside, which makes the membrane come down on the inside, creating an aperture.

A small quantity of oil based ferrofluid has been tested in Optotune and directly showed that the viscosity is much too high create a clear aperture on the glass. Water based Ferrofluid could not be used as it would evaporate through the membrane.

Fig. 16 Ferrofluid on glass plate above permanent magnet

Fig. 16 shows Ferrotec S12n on a glass plate, lying on a magnet. From the picture we can see that the fluid is too viscous and therefore too slow to creep to the magnetized area. Also the aperture in the middle is still brown. Waiting until the aperture clears up takes long (>> 1 minute).

3.8.3 Electromagnetic: coil actuator

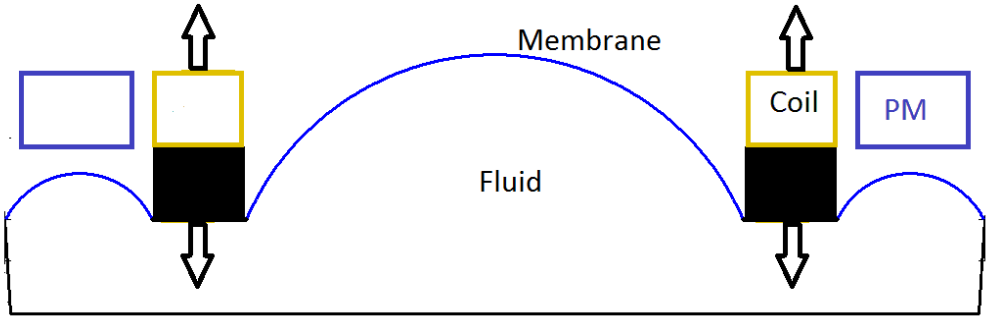

Fig. 17 Optotune coil actuator design

The coil actuation principle is used in Optotune's electrical lenses. In Fig. 17, the orange part in the picture resembles a permanent magnet. The yellow part is a coil wounded around the bobbin. The bobbin is glued onto the membrane and is able to move vertically. When a voltage is applied on the coil, the bobbin will move.

3.9 Liquid selection

Various tests have been performed to identify suitable fluids for the aperture.

Qualitative goal of liquid selection

To select a liquid having

- light absorbing properties (black)
- a fast escaping action from the glass – membrane contact region
- no toxicity
- temperature specification fitting operating temperatures requirements
- compatibility with membrane and casing

Identification of qualitative specification

- Light absorbing properties
    - Fluid either being black or being able to solve a colorant, for example:
        - Oil based black ink
        - Food colorant powder
        - Carbon black powder
- A fast escaping action from the glass – membrane contact region
    - Surface tension: when the surface tension of the liquid is higher than that of the surface, the liquid will not stick onto the surface. The higher the surface tension, the faster the liquid will flee away
    - Viscosity: the lower the viscosity, the quicker the fluid will be able to move away from the contact region
- No toxicity
    - No irritation to skin, eyes
    - No swallowing risk
    - No environmental damage
- Temperature requirements
    - Stable region: [-40 , +85] degC
    - Operation region: [-20 , +65] degC
    - No evaporation of fluid
        - Low vapor pressure: <1 atm for whole Temperature range
        - High boiling point: > 85 degC
    - No combustion: high flash point: > 85 degC
    - Stable mass: not hygroscopic
- Compatibility with membrane and casing
    - Does not solve the silicone membrane and/or casing plastics
    - Does not leave drops on the membrane

Proposed test methods

- Surface tension, viscosity
    - Pressure test by sandwiching a dark fluid between glass and membrane. As the membrane is pressed on to the glass, the speed with which the fluid moves away from the pressure area becomes visible. Also, one can see the clarity of the aperture area. As higher the surface tension and as lower the viscosity, the better the result will be.
- Light absorbance
    - Test compatibility with dyes and pigments
- High temperature stability, high boiling point, low vapor pressure
    - oven test: 85 degC, 48 hours
- Low temperature stability, low melting point
    - fridge test: -30 degC, 48 hours

Properties of typical liquids

- Water (dyed black)
    - Lipophobic: water escapes from the lipophilic silicone membrane
    - Surface tension: 72 mN/m is very high and therefore the water flees away quickly
    - High temperature stability: Water evaporates over time
- Oil based ink
    - Dries out (fluid evaporates)
    - Low surface tension, sticks to surface
- OL0907 (used for 1st Manual Lens aperture demonstrator)
    - Surface tension marginally good, not high enough
    - High viscosity
- OL0904
    - All properties ok, but forms drops on the membrane when heated
- OL0903
    - All properties ok, but is too aggressive to use together with plastics
- OL 0901
    - Melting point = -6 degC. All other properties are ok
    - Surface tension 31 mN/m
- **OL0902 (favorite fluid)**
    - Melting point = -6 degC. All other properties are ok
    - Surface tension 36 mN/m

Testing fluid OL0902 with black dye

- **Using oil based ink**
    - Decrease in surface tension because of ink mixture. Ink has a low surface tension in order to wet the paper
    - Filtering the ink mixture with 0.2 μm increases the surface tension, but also decreases the opacity

3.10 Feasibility demonstrators

To investigate the functionality of the aperture principle, several demonstrators are made. The technique for the demonstrators is shown in 3.3.

3.10.1 Manual aperture demonstrator 1

- goal
  - Test functionality of aperture principle
- transparent fluid
  - OL0907
- ink
  - Pelican oil based black ink (15 ml)

Fig. 18 Aperture demonstrator shows a black spot in the center

Results

- As shown in this picture, some fluid is trapped in the center
- A small particle appears to be right in the middle, allowing other fluid particles to stay in this region
- The intensity of the spot depends on the speed with which the ML was opened

Possible improvements

- Decrease concentration of ink
- Filter ink particle size

3.10.2 Manual aperture demonstrator 2

- goal
  - Solve 'trapped fluid' problem
- transparent fluid
  - OL0902 (identified fluid from liquid selection)
  - higher surface tension: 36mN/m
  - lower viscosity
- ink
  - Pelican oil based black ink (3 ml)
- mixture filtered with 1mu filter

Fig. 19 Aperture demonstrator 2

Results

- the spot, seen in demonstrator 1, is gone
- optical region in center shows a lens effect
  - optical region is not flat
  - the quality of the optical region depends on speed of opening the aperture
- the fluid is transparent at the side of the transparent region
  - not enough ink applied
  - lens effect on the aperture edge

Proposed improvements

- deposit silicone layer on glass plate
  - a Silicone layer / selected coating will create a lower surface energy
  - fluid will flow away faster
- try with more drops of ink (2-3 instead of 1)
  - fluid will be less transparent on the sides

3.10.3 Manual aperture demonstrator 3

- goal
  - test influence of surface tension on trapped fluid problem
- transparent fluid
  - H_2O(l) distilled
  - higher surface tension: 72mN/m
  - lower viscosity
- ink
  - Allura Red (food colorant)
- membrane
  - SE0904-017 6/7/8
  - t0 = 222μm, t1 = 102 μm
  - prestrain: 48%
- glass
  - Silicone coated (SE0904) layer

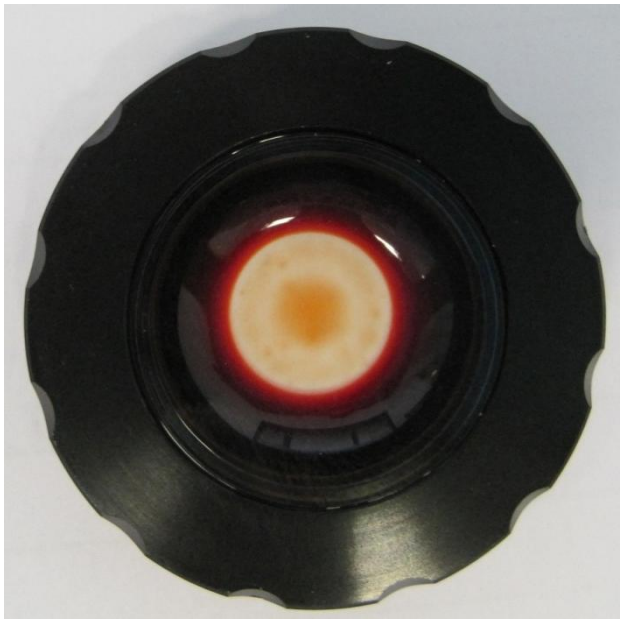

Fig. 20 Demonstrator 3 built with water and red colorant

Results:

- just a high surface tension is not enough to make a clear aperture in the Manual Lens demonstrator
- again, the clarity of the aperture depends on the speed with which the membrane is moved down

3.10.4 Manual aperture demonstrator 4

- goal
  - Test influence of contact angle on trapped fluid problem
- transparent fluid
  - OL0902 (6.6544 g)
- ink
  - Pelican oil based black ink (0.1297 g)
  - 0.9009 g of mixture filled
- bottom glass
  - Lens convex curved bottom glass to increase contact angle with membrane

Fig. 21 Demonstrator 4 built with a lens as bottom glass

Results:

- The trapped fluid in the middle remains and creates extra convex lens
- Depending on the transparency of the fluid, the outer region will act as a concave lens
- Increasing the contact angle has no significant influence on the trapped fluid

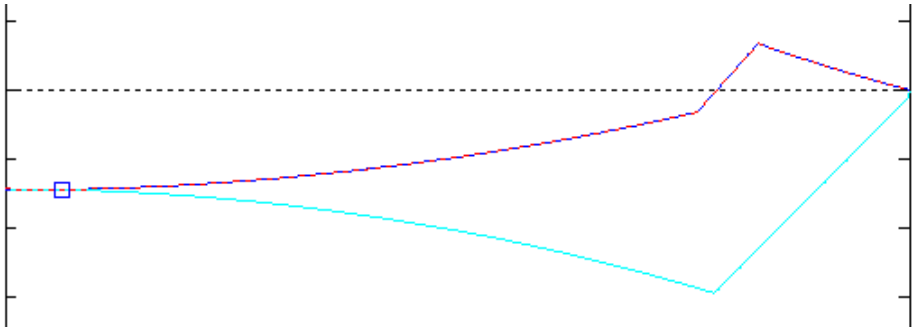

Fig. 22 Simulation of bottom contact angle (made with Matlab tool 'shape predictor')

3.10.5 Positive pressure experiment

From earlier experiments, it is reasonable to conclude that to create a negative pressure in the fluid will not result in a clear aperture. There might be too little force pushing the fluid away from the aperture area. A discussion about the trapped fluid can be found in 3.12. In search of a working method, experiments have been performed with a positive pressure on the fluid. This type of actuation might be able to push the liquid away and create a clear aperture. The next picture shows a 3d cross section of the experimental setup.

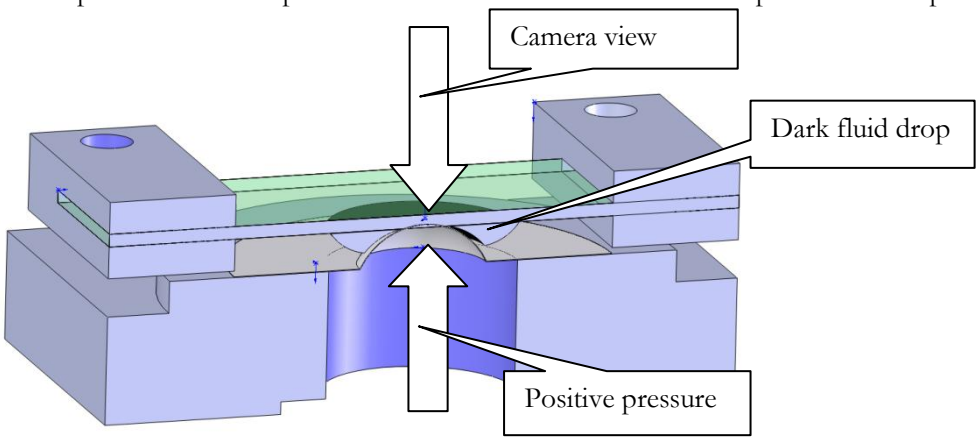

Fig. 23 Positive pressure experimental setup

The air pressure underneath the membrane bulge is controlled manually with an air pressure regulator. The bulge pushes up against a drop of fluid. As the bottom of the air chamber is closed by a cover glass, light from underneath can be shined through the created aperture. The bulge creates an aperture on the glass by pushing away the fluid. The next pictures, taken with a microscope camera, show the results.

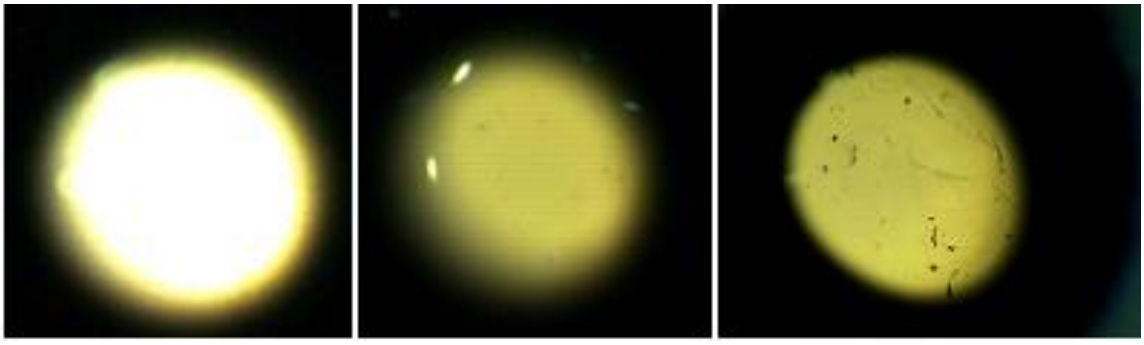

Fig. 24 (a,b,c) Test results with positive pressure. Picture c shows dirt on the membrane. The test setup is in open air, therefore the membrane is never completely clean. A picture with trapped fluid in the center is not available.

Several experiments have been done with this test setup. The following conclusions are made:

- A low concentration of ink with small particle size can produce a optical transparent area
- A higher concentration of ink does create a dark spot in the center (no picture available)
- A bigger particle size creates a dark spot in the center
- It is not confirmed that there is no lens effect in the center
- The aperture edge is not sharp

3.10.6 Manual aperture demonstrator 5

To investigate how the positive pressure discussed in the previous section performs in a closed membrane setup, a new demonstrator is being made based on the manual lens design. However, to create a positive pressure, the design is somewhat changed by inserting a second lens shaper.

Fig. 25 shows the simulation of the double liquid design made by the Shape Predictor (Matlab tool, see 4.4). Two containers are put on top of each other, with different fluids, separated by the membrane (blue). As the top container moves down into the bottom container, a bulge is created that presses onto the glass plate.

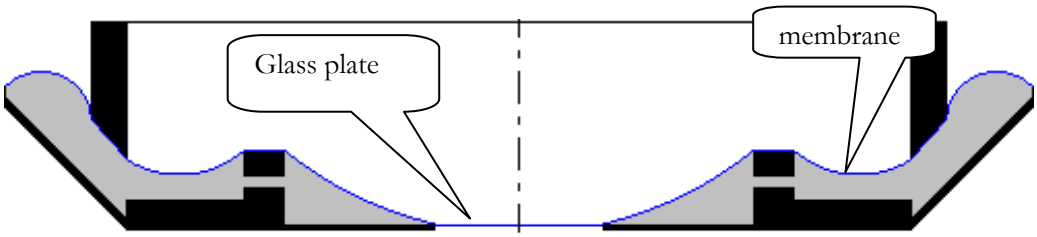

Fig. 25 Simulation of the positive pressure lens created in Matlab tool 'Shape Predictor'

The simulation has been used to calculate the fluid volume in the top and bottom containers.

The volume of top and bottom fluid is very critical, because it determines the possibility to create an aperture and changes the height of the outer membrane ring. With the wrong amount of fluid, the range of the setup is very limited.

By using matching refractive indexes of the fluids, the lens effect in the aperture edge and in the center are solved.

Results

Fig. 26 Double liquid demonstrator shows the typical black circle

Again, the demonstrator showed the black circle. The fluid has not been filtered well enough and contains visible black particles.

3.11 Troubleshooting

Several actions have been undertaken in order to solve the dark circle problem we have seen in previous sections. To summarize the various attempts and their arguments, Tbl. 1 is shown underneath. Properties of the demonstrator setup are described and argumentation for and against their influence are shown.

As the various properties create a multidimensional space of possible combinations, the demonstrators were designed to, as good as possible, test the influence of the single property.

The last mentioned solution "Slots in glass" is yet to be tested.

Solution to 'trapped fluid'	Arguments pro	Arguments contra
Surface tension Hydrophilic/phobic	Flatter drop means higher likelihood to form dark circle	- Tested with water, stain stayed - Only mercury is higher
Viscosity	High inertia of fluid will have the fluid stay in the middle	- Tested with water, stain stayed
Colorant Particle Size	Smaller colorant decreases viscosity and flows away quicker	- colorant travels through membrane (in double liquid setup)
Contact angle	Higher 'zip angle' between membrane and glass will push away fluid	Tested with lens bottom glass, dark stain appeared
Concentration	Lower concentration of dark fluid will make stain less visible	Softer aperture edge, higher edge lens effect
Slots in glass (not yet tested)	Fluid can flow away from center through slots in glass	Optical effect of slots

Tbl. 1 Troubleshooting table

3.12 Trapped fluid discussion

Several experiments are done while trying to solve the trapped fluid problem. A critical view on this problem is presented in this section.

Regarding the fluid, the current design is very limited by the use of transparent liquids used by Optotune. To identify a fluid having the correct properties for long term use in the membrane setup requires a lot of time. The used fluids are not necessarily compatible with the pigments and a better combination of pigment and fluid could be found.

The functionality of the aperture has not proven to ever completely solve the trapped fluid problem. The question "Would the aperture of a demonstrator with transparent liquid show a completely flat aperture region?" cannot be answered. The suspicion is though, that it would not. The possibility to measure the aperture surface height of a demonstrator with transparent fluid exist and would give an answer. The answer given by this experiment would only apply to one fluid, so more fluids should be experimented with. However, each demonstrator costs money and time and there was no time left for this experiment.

3.13 Conclusions on aperture design

Lens technologies developed at Optotune are based on silicone circular membranes. Such a membrane encloses a container of optical fluid and is able to change its surface. This principle has the potential to be used as an optical aperture. With little mechanical components, such an aperture could be made small and cheap.

A silicone membrane in 2d axisymmetric circular setup is pulled down to a glass plate, as a result of hydrostatic underpressure. The volume between the glass plate and the membrane is filled with a dark fluid.

- The contact region creates an optical aperture, the size of which can be changed.
- The contact region shows not to be completely transparent. A dark circle forms on the glass plate.

The dark circle problem could not be solved by

- increasing surface tension of the dark liquid
- adjusting Hydrophilic / Hydrophobic characteristics.
- Increasing the contact angle between the membrane and the dark liquid
- Applying a negative or positive pressure

Two methods having a positive influence on the dark circle are identified:

- Decrease of concentration of black particles
- Decrease of size of black particles

However, applying these methods has disadvantages:

- Soft aperture edge with lens effect
- Curvature of membrane (lens effect) in the center

The lens effect in the aperture edge and center can be solved by using a double liquid setup with matching refractive length. Though, also this setup has its disadvantages:

- More complicated to produce
- Takes up more size
- Pigment leaks through the membrane from the dark fluid to the transparent fluid.

3.14 Aperture Outlook

In order to design a functioning tunable aperture, I have the following recommendations.

- Measure optical surface shape of the aperture region of a single liquid demonstrator
    - Fill the demonstrator with Optotune's transparent optical fluid, no added pigment
    - Use various tuning speed
    - Conclude whether the aperture region shows a lens shape
    - Investigate influence of fluid type and properties on surface shape
    - Later on, add pigment and perform the same test
- Experiment with micro slots in the bottom glass
    - Fluid can escape from the aperture region through the slots
    - Measure surface shape of aperture region

4 Membrane model identification

Optotune designs lenses based on silicone elastomer membranes. The membrane, being placed in an axisymmetric setup, functions as a lens when a pressure underneath the membrane is applied and a bulge forms. The pressure is applied through an optical fluid. After choosing a silicone elastomer material (SE0904), the membrane can be dimensioned by choosing a membrane thickness, applying a certain prestrain and choosing an aperture radius of the circular setup.

A complex part of the design phase of a lens comprises the calculation of the deflection of the membrane at a combination of previously mentioned parameters. From the deflection of the membrane and the fluid's refractive index, the focal length of the lens can be calculated. Finding the influence of thickness, prestrain and aperture radius on the deflection of the membrane is important for two reasons:

- Motor size design; calculate maximum needed force on the lens shaper depending on membrane parameters
- Design of membrane production ; what is the production sensitivity to changes on membrane parameters

The influence of the membrane parameters on the deflection will be measured experimentally in this section. A measurement setup is designed, able to test membranes having various properties. Later on, these measurements will be simulated by material models.

Results of this section will be used for the mechanical design of lenses. The experiments will be done on deflections in the center. The optical shape will not be covered in this research. In optical design, surface accuracy needs to be < 1 µm, where in mechanical design, the surface is only determined by the center of the bulge and is approximated as a perfect sphere.

This research only investigated using the material SE0904. Research methods could readily be applied to other materials.

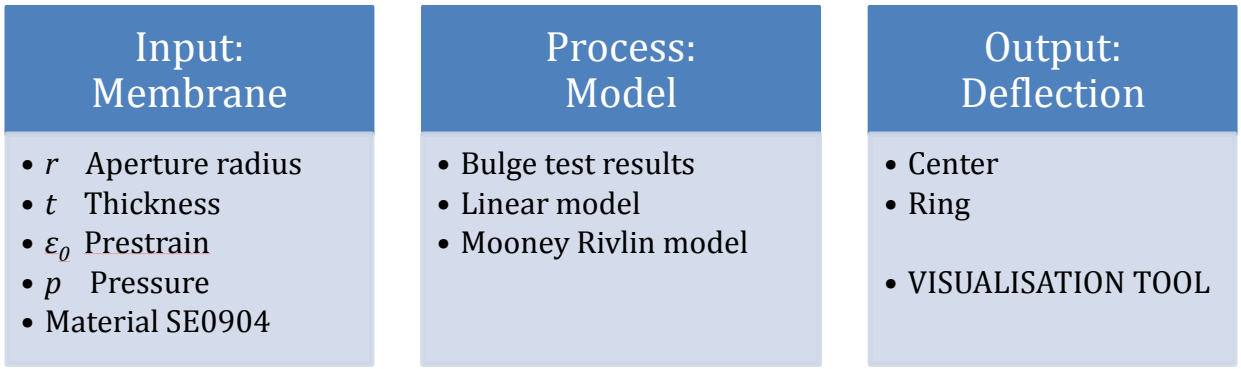

Fig. 27 Overview of membrane material problem

In Fig. 27, the membrane material problem overview is given. Every combination of input parameters gives a different output as center deflection and ring deflection. The method to get the deflection values can be through experiments with bulge tests, through a linear model (Rosset, 2009) or with the Mooney Rivlin material model. To visualize the results, a visualization tool has been developed in MATLAB®. The tool is able to display various geometrical setups for various Optotune lens designs, based on the material models derived in this thesis.

4.1.1 Center and ring distinction

To calculate the stress in the membrane, a model based on a spherical pressure vessel is shown in this section. Measurements done at Optotune (Graetzel, 2009) show that the contour of a blown up membrane resembles the shape of a sphere.

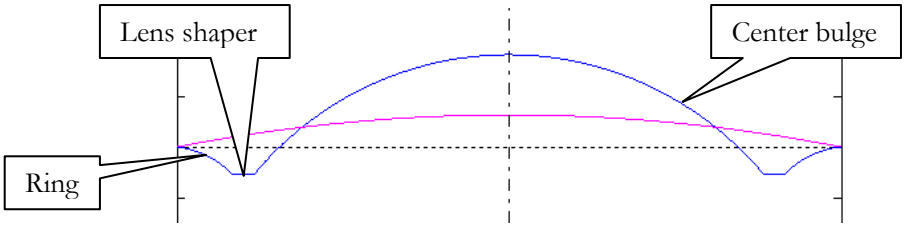

Fig. 28 Shaped membrane in bare lens setup (pink) and single lens shaper setup (blue)

In Fig. 28, a two dimensional plot containing two membrane setups is shown. The first line (pink) shows a membrane slightly blown up because of a positive hydrostatic pressure in the fluid beneath the membrane. If one pushes a 'lens shaper' onto the membrane, the center comes further upwards and the side next to the lens shaper shapes accordingly. The shape on the other side of the lens shaper will be referred to as 'ring'.

4.1.2 Experiment design

The membrane is clamped between two metal plates. A distributed force is applied by magnets, clamping the plates together. The membrane and plates setup closes a pressurized cylindrical container with a pressure sensor. The setup is held in place by a threaded ring.

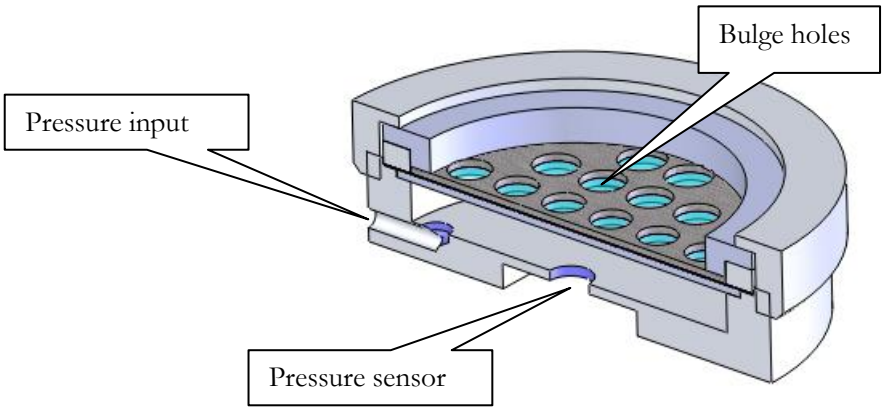

Fig. 29 Cross section of deflection versus pressure test setup.

4.1.3 Measurement devices and accuracy

The air pressure is supplied by a manual pressure regulator, type Bellofram T41. The pressure is measured by a digital pressure sensor, type Intersema MS5803. The accuracy of the pressure sensor is 10 Pa. The height of the bulge is measured by a Werth multisensor coordinate measurement machine. The maximal inaccuracy of the measurement machine is 5 µm. To obtain these accuracies one needs to monitor the pressure over time to insure the regulator keeping constant pressure.

Fig. 30 Measurement devices: Multisensor Coordinate Machine, Pressure Regulator, Pressure Sensor

4.1.4 Description of legend for measurement plots

Each measurement plot has a legend. The explanation for the legend is given in Fig. 31. The measurement ids are the ids stored in the measurement database.

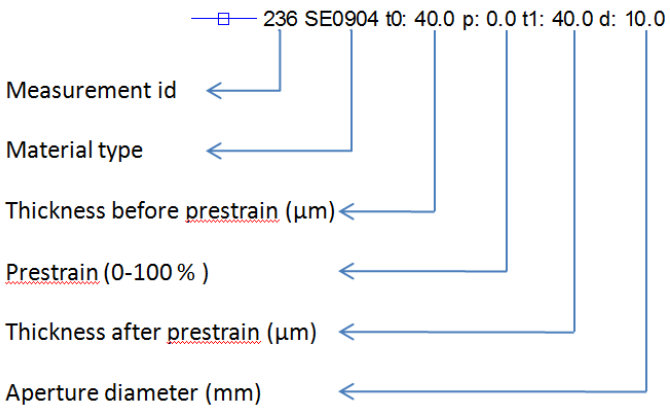

Fig. 31 Explanation of measurement legends

4.2 Bulge measurements

The word 'bulge' is often used to describe a deflected circular membrane. In this report, a distinction is made between the bulge shape and the ring shape (Fig. 28).

4.2.1 Deflection versus pressure – influence of radius

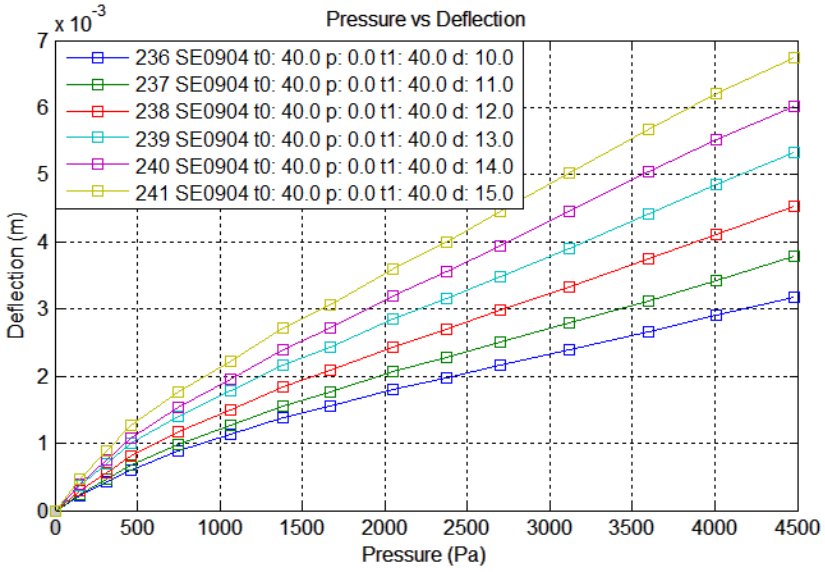

Fig. 32 Measurement of single membrane with varying aperture diameter

In Fig. 32, the deflection versus pressure measurement of a 40 µm SE0904 membrane without prestrain is shown. This measurement shows that when the aperture diameter is increased, the deflection increases. As the aperture area grows quadratically with respect to diameter, it can be shown that deflection can be normalized to aperture area ($A = \pi r^2$), as seen in Fig. 33.

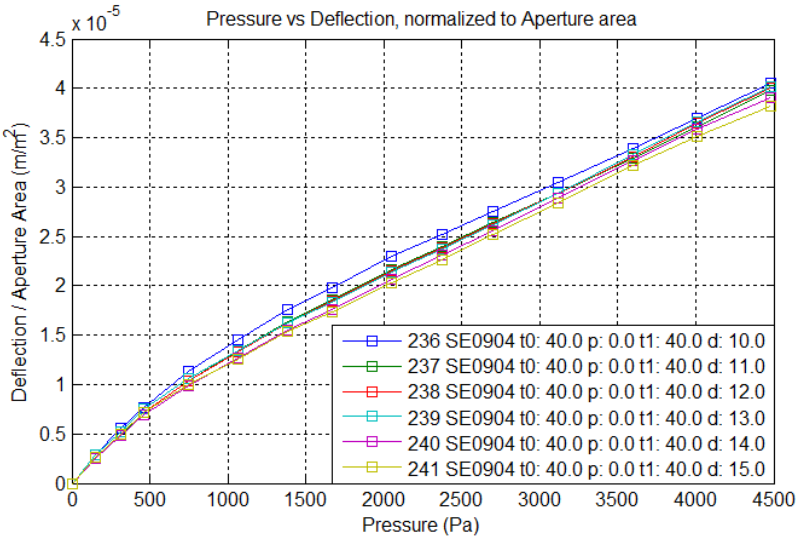

Fig. 33 Deflection versus pressure measurement, normalized to aperture area

4.2.2 Deflection versus pressure – influence of prestrain

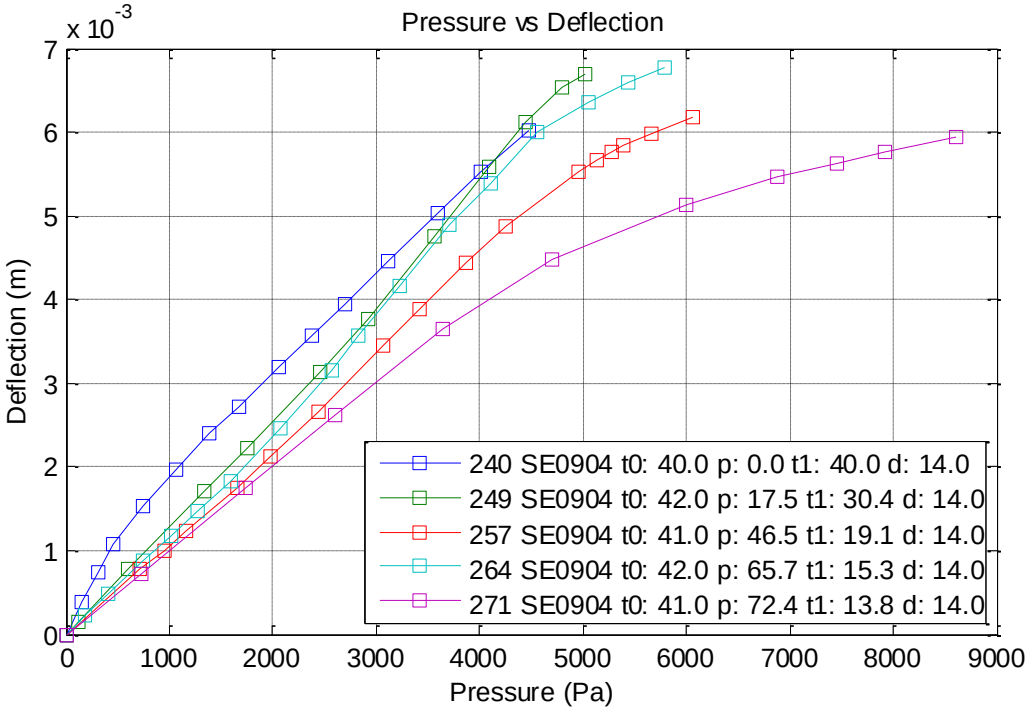

Fig. 34 Deflection versus pressure measurements – influence of prestrain

In Fig. 34, several deflection versus pressure measurements are showed. All used membranes are from the same production batch and plate. The aperture radius is kept constant and thickness before prestrain (t0 in the legend) is nearly identical. The only varied parameter is prestrain and therefore also thickness after prestrain. Several observations have been made.

- The nonzero prestrained membranes have a linear start region
- The more prestrain, the stiffer the membrane
- At higher deformation, the nonzero prestrained membranes can become weaker than the zero prestrained membrane due to a steeper slope

4.2.3 Simulation approach

To simulate the deflection versus pressure measurements, the stress strain behavior of the membrane material needs to be identified. A material model will be fitted to the stress-strain curve and this fit can be used to simulate deflection versus pressure experiments. However, due to the membrane stretch not being constant over the cross-section of a bulge (Fig. 35)(Rosset, 2009), choosing the strain and thickness to use for the stress will influence the stress-strain curve. Three stretches are chosen in this report.

- Stretch at the pole (center) of the membrane bulge
- Stretch over the arc length of the cross section of the bulge
- Stretch over the surface increase of the bulge

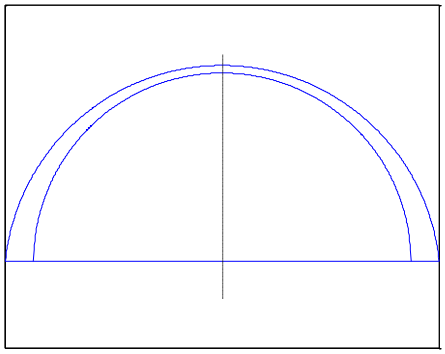

Fig. 35 Thickness, and therefore stretch, changes through the cross section of the bulge. The outside of the bulge only experiences uniaxial strain, the middle experiences biaxial strain

4.2.4 Thickness, stretch and strain in equibiaxial setup

Silicone elastomer material is often modeled as incompressible (I. M. Ward, 2004). This assumption implies a Poisson ratio of $\nu \approx 0.5$ and that the volume remains constant as used in Eq. 1.

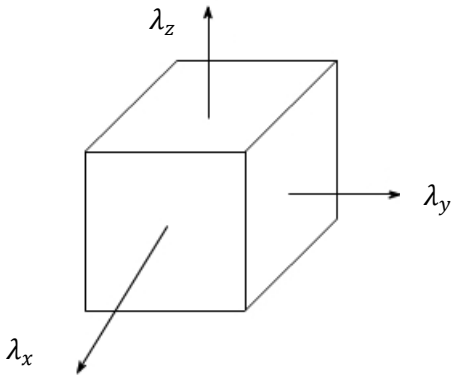

Fig. 36 principle directions of stretch

$$\lambda_x \lambda_y \lambda_z = 1 \quad \text{Eq. 1}$$

$$\lambda = \frac{l + \Delta l}{l} = \varepsilon_x + 1 \quad \text{Eq. 2}$$

Eq. 2 explains the relation between stretch and strain. Both are used in various applications where one of both leads to simpler formulas.

In equibiaxial setup, thickness of the membrane and stretch (and therefore strain) are linked. The relation is given in the following calculations. Note, $\lambda_x = \lambda_y = \lambda$ in equibiaxial setup. $\lambda_z$represents the stretch in thickness direction.

$$V_0 = V_1 \rightarrow A_0 t_0 = A_1 t_1 = A_0 \lambda_x \lambda_y t_1 \quad \text{Eq. 3}$$

$$t_1 = \frac{t_0}{\lambda^2} \quad \text{Eq. 4}$$

4.2.5 Bulge radius

The next step is to link the deflection of the sphere, which in the end determines the focal length of the lens, to a new spherical radius R. This is needed to apply the formula for a complete vessel, to a slightly deflected bulge.

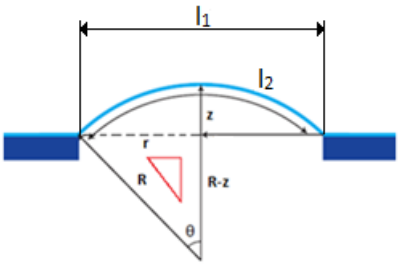

Fig. 37 Geometry of spherical bulge

From the geometry as depicted in Fig. 37, one can create Eq. 5.

$$R^2 = (R - z)^2 + r^2 \quad \text{Eq. 5}$$

Rewriting of Eq. 5 leads to:

$$R^2 = R^2 - 2zR + z^2 + r^2 \quad \text{Eq. 6}$$

$$R = \frac{z^2 + r^2}{2z} \quad \text{Eq. 7}$$

4.2.6 Stretch of arc length

The stretch in the membrane can be approximated by the stretch over the arc length of the membrane's cross section. The arc length of a spherical cap is calculated as follows.

$$\theta = \sin^{-1}\left(\frac{r}{R}\right) \quad \text{Eq. 8}$$

$$l_1 = 2r \quad \text{Eq. 9}$$

$$l_2 = 2R\theta = 2R \sin^{-1}\left(\frac{r}{R}\right) \quad \text{Eq. 10}$$

$$\lambda_{arc} = \frac{l_2}{l_1} = \frac{R}{r} \sin^{-1}\left(\frac{r}{R}\right) \quad \text{Eq. 11}$$

$$0 < z < R: \qquad \lambda_{arc} = \frac{l_2}{l_1} = \frac{R}{r}\sin^{-1}\left(\frac{r}{R}\right)$$
$$R < z: \qquad \lambda_{arc} = \frac{l_2}{l_1} = \frac{R}{r}\left(\pi - \sin^{-1}\left(\frac{r}{R}\right)\right) \qquad \text{Eq. 12}$$

As the deflection becomes bigger than the bulge radius, a correction is needed as seen in Eq. 12.

4.2.7 Stretch in bulge center

The stretch in the center can be measured by painting four dots in the center of the circular membrane. When the pressure is increased, the measured distance between each couple of dots leads us to the stretch in the center.

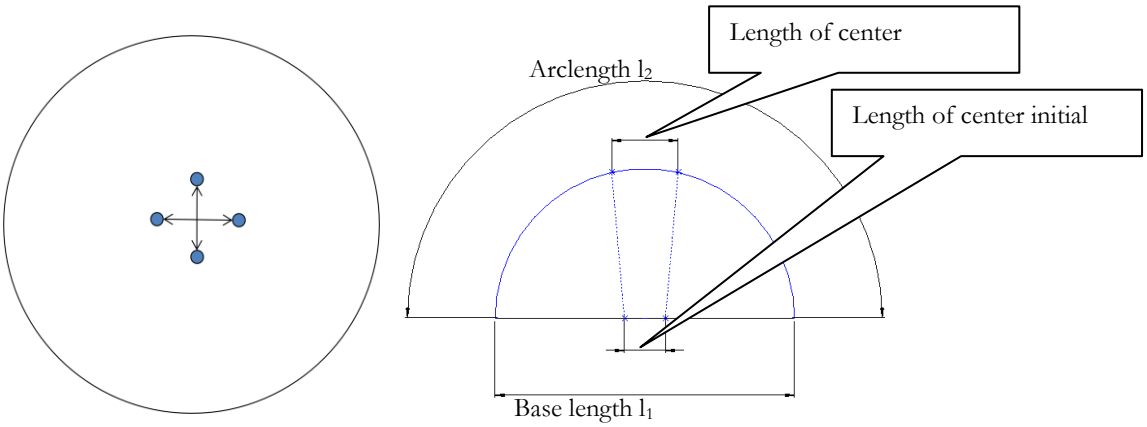

Fig. 38 Biaxial stretch measurement, measuring distance between dots in center.

The objective of measuring the stretch in the center is to use it for determining stress in the membrane. The stretch in the center leads us to the thickness in the center (4.2.4). This thickness can be used in the vessel function.
A linear relation has been found between the measured stretch in the center and the arc length stretch. The arc length stretch is the ratio l_2/ l_1 as shown in Fig. 38 and can be calculated directly from the measured deflection height in the center. This relation is independent of thickness, prestrain and aperture diameter of the membrane. Furthermore, it shows that it is not necessary to do biaxial measurements anymore, these can be predicted with only the height measurement.

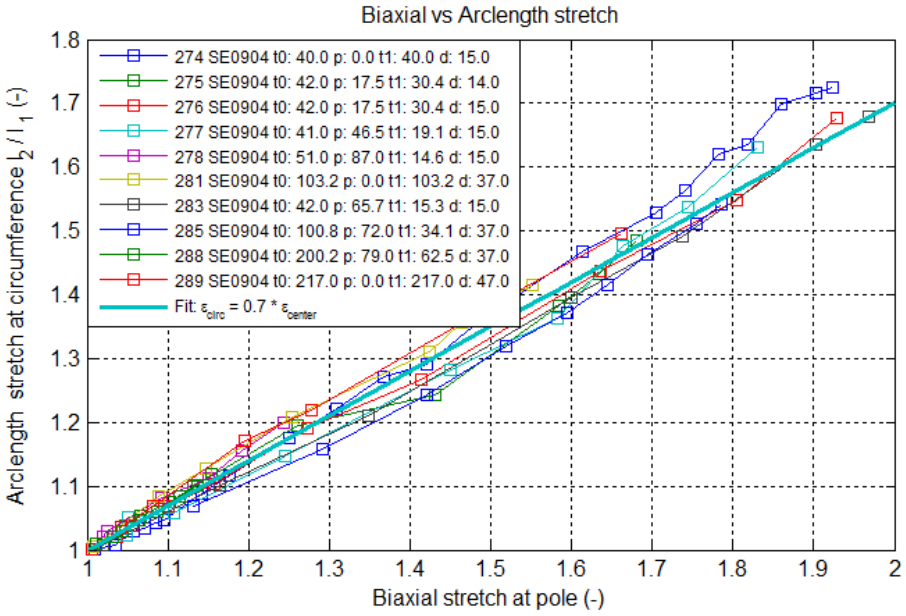

Fig. 39 linear relation between arc length stretch and stretch in the center

The fitted relation is given in Eq. 13. Please note, the relation is found completely empiric and has no physical explanation so far.

$$\varepsilon_{arc} = 0.7 \cdot \varepsilon_{center} \quad \text{Eq. 13}$$

$$\lambda_{arc} = 0.7 \cdot (\lambda_{center} - 1) + 1 \quad \text{Eq. 14}$$

The error on the fitted line is plotted in Fig. 40. No specific pattern has been found. The legend is kept the same as in Fig. 39.

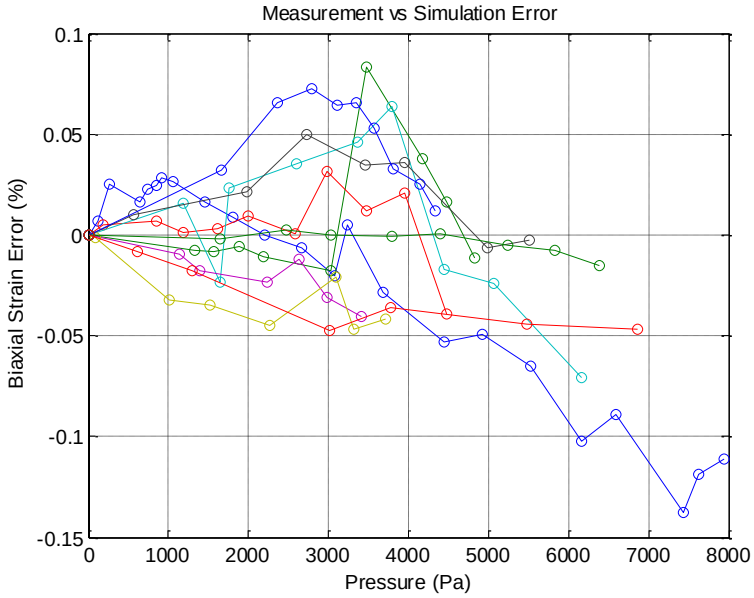

Fig. 40 Error made in relation to fitted line.

4.2.8 Stretch of surface

In the last section, a relation has been found between the stretch in the center of the bulge and the stretch over the arc length of the bulge. In this section, a new stretch will be introduced based on constant volume and the stretches will be compared.

Stretch with constant volume

The membrane's deformation into a spherical cap will increase its area, and due to the constant volume properties of elastomer this will lead to a decrease of the membrane's thickness (Rosset, 2009):

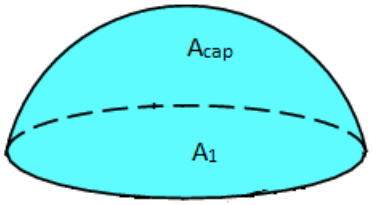

Fig. 41 Surface area of bulge in flat and in blown-up state

$$\lambda_x \lambda_y \lambda_z = 1 \qquad \text{Eq. 15}$$

$$\lambda_z = \frac{A_1}{A_{cap}} = \frac{\pi r^2}{\pi(r^2 + z^2)} = \frac{r^2}{(r^2 + z^2)} \qquad \text{Eq. 16}$$

$$\lambda_z = \frac{1}{{\lambda_{cap}}^2} \rightarrow \lambda_{cap} = \sqrt{\frac{(r^2 + z^2)}{r^2}} \qquad \text{Eq. 17}$$

4.2.9 Stretch comparison

In Fig. 42, the various stretches calculated in previous sections are shown. Later on, these stretches are used to calculate thickness and eventually stress. Stretch in the center is calculated by the empirical Eq. 14. Arc length stretch is calculated by the analytical Eq. 12. Surface stretch is calculated by the analytical Eq. 17. Comparing the stretch over arc length and surface showed $\varepsilon_{surface} \approx \varepsilon_{arc} \cdot 0.7$.

Fig. 42 presents the three stretches. All three can now be calculated from the known z-height, given a spherical model. The stretches can later be used to calculate a thickness.

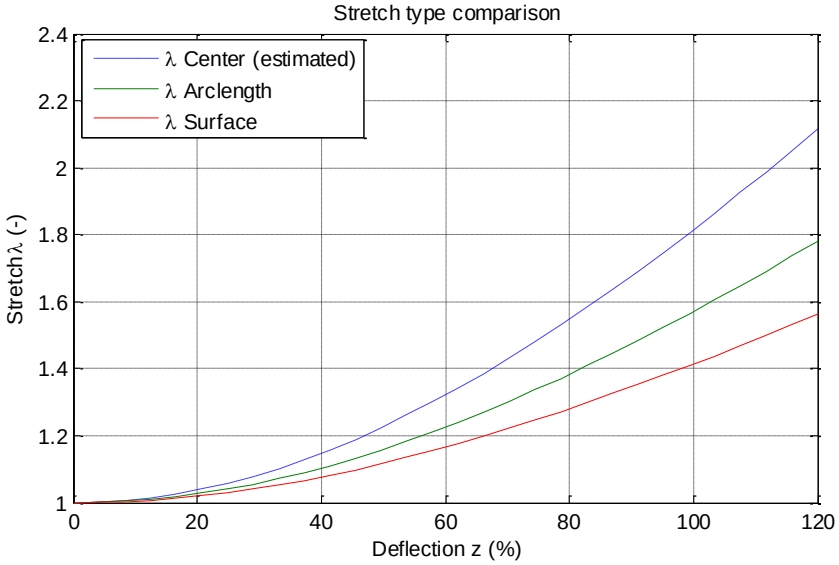

Fig. 42 Stretch comparison: stretch versus deflection as percentage of half sphere.

4.2.10 Bulge thickness calculation

In order to calculate the stress in the bulge, which will follow later this chapter, the thickness needs to be determined. As the thickness of the bulge is not constant over the cross section, one needs to approximate the thickness to use it later in stress calculations. The previously calculated stretches each have their own thickness.

$$t_1 = \frac{t_0}{\lambda_{prestrain}^{\ 2}} \quad \text{Eq. 18}$$

$$t_{2,center} = \frac{t_1}{\lambda_{center}^{\ 2}} \quad \text{Eq. 19}$$

$$t_{2,arc} = \frac{t_1}{\lambda_{arc}^{\ 2}} \quad \text{Eq. 20}$$

$$t_{2,surface} = \frac{t_1}{\lambda_{surface}^{\ 2}} \quad \text{Eq. 21}$$

4.2.11 Stress calculation

The center is modeled as a spherical vessel. Consider a vessel under static equilibrium with a spherical surface. Newton's first law of motion states the stress around the wall must have a net resultant force that equals the internal pressure across the cross section.

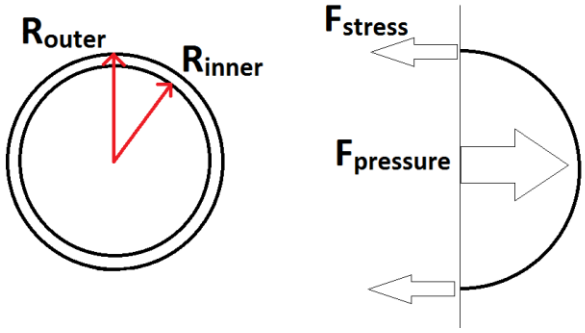

Fig. 43 Spherical vessel: F_{stress}=$F_{pressure}$

As clarified in Fig. 43, the resultant force from stress in the membrane must equal the force resulting from the pressure in the fluid (see Eq. 14).

$$F_{stress} = F_{pressure} \quad \text{Eq. 22}$$

Now to specify the force resulting from stress in the membrane:

$$F_{stress} = \sigma\, A_{wall} = \sigma 2\pi t R \quad \text{Eq. 23}$$

In Eq. 23, the following derivation for A_{wall} has been used:

$$A_{wall} = \pi\left(R_{outer}{}^2 - R_{inner}{}^2\right) = \pi\left(R_{outer}{}^2 - (R_{outer} - t)^2\right)$$
$$A_{wall} = \pi\left(R_{outer}{}^2 - R_{outer}{}^2 + 2tR_{outer} - \cancel{t^2}\right)$$
$$A_{wall} \cong 2\pi tR$$

Eq. 24

In Eq. 24, the square of thickness t is negligible when assuming a thin sheet.
Now to calculate the resultant force from the pressure inside the vessel. The resultant force must equal the force over the cross section, so we obtain:

$$F_{pressure} = p\,A_{cross} = p\,\pi R^2$$

Eq. 25

Combining Eq. 23 and Eq. 25 enables us to express the stress as function of the pressure.

$$\sigma = \frac{pR}{2t}$$

Eq. 26

4.2.12 Calculated stress strain curve and Mullins effect

The stress in the membrane can be calculated using Eq. 26 and will characterize the membrane material. Later on, the stress strain curve will be fitted and used to predict deflection versus pressure curves.

To calculate the stress from the deflection versus pressure measurements, we use the vessel formula Eq. 26. The pressure 'p' is given by the measurements. The radius 'R' is calculated directly from the measured deflection height. The thickness 't' shall be measured at the base of the bulge. As at the base the membrane has an extreme curvature and there is no space to measure thickness, the thickness has to be approximated.

As shown in 4.2.9, the average strain over the arc length is a factor 0.7 of the strain in the center. Therefore, **the thickness is not constant over the membrane arc**. Three thicknesses have been identified in previous sections. The thickness in the centre is used for the stress strain calculations, as this thickness showed the best fit (stress strain curves had the most overlap).

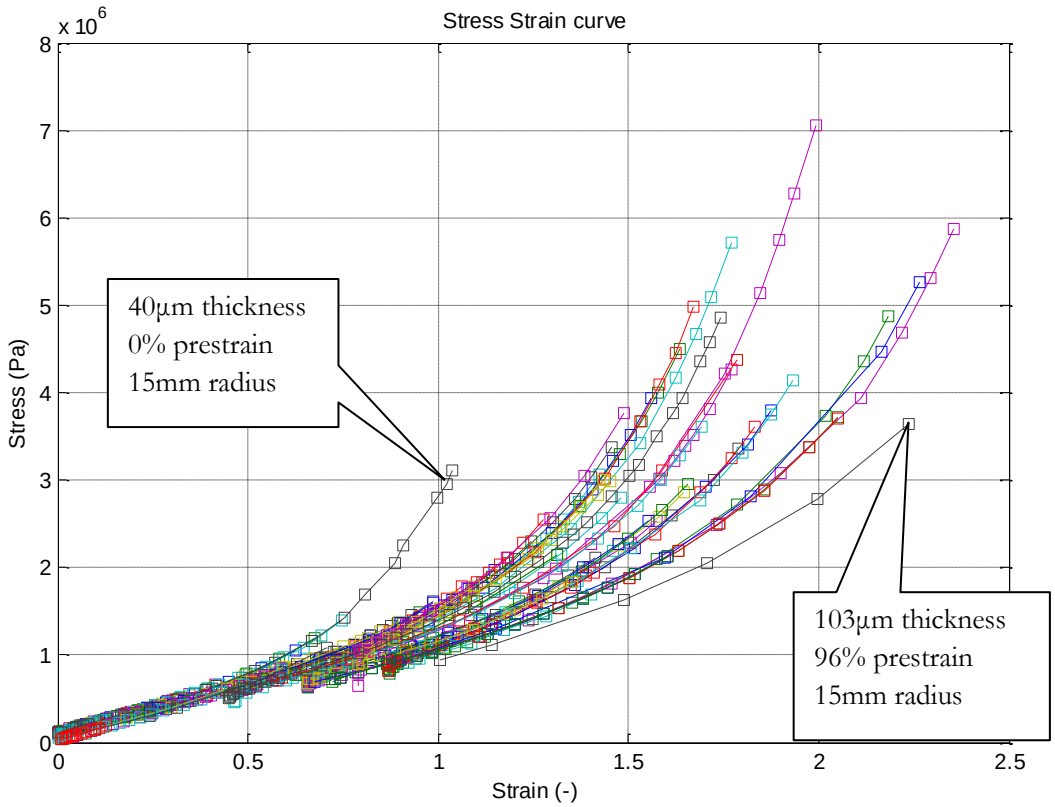

Fig. 44 Stress strain curve based on thickness in center

Stress strain plot

Fig. 9 shows the stress strain calculated from various membrane measurements. Measurements that start at a higher strain have a nonzero prestrain. The figure shows stress strain for measurements with membranes having various thicknesses, diameters and prestrains. Each line represents the stress strain calculated from a single membrane. Each point is calculated from a deflection versus pressure measurement.

Mullins effect

The stress strain curve should represent one material model. All stress strain curves should align into one curve. The cause of having various branches when reaching higher strain might be the Mullins effect. The Mullin's effect states that the stress strain curve of a hyperelastic material depends on the highest strain the material ever experienced. If an elastic band is bent once to a large extent, it will behave weaker than before.

The unknown parameter is the maximal strain that the membrane has experienced during production. To produce a membrane with prestrain, a membrane is stretched much further than necessary. During this process the membrane might weaken.

Measurement tool and placement effect

Fig. 45 shows a measurement performed with the measurement tool in Fig. 46. The yellow line, representing the 15mm diameter bulge, clearly behaves weaker in the deflection versus pressure than the other, smaller apertures. This behavior is also visible in the calculated stress strain plot. This effect is visible in every membrane tested with this tool, except for the membrane with no prestrain, shown in Fig. 47.

The explanation for this effect lies in the prestrain procedure. The 15mm aperture is designed in the center of the measurement tool. As we have seen in section 4.2.9, the center of a membrane bulge stretches much more than the average stretch. Therefore, the Mullin's effect in the center after prestrain is much higher than in the outer parts of the membrane. Because there is more Mullin's effect in the center, the center will behave weaker afterwards.

One could argue that the middle of the measurement tool moved up after applying pressure and influenced the measurement. This is not the case, since in Fig. 47 we cannot see any offset.

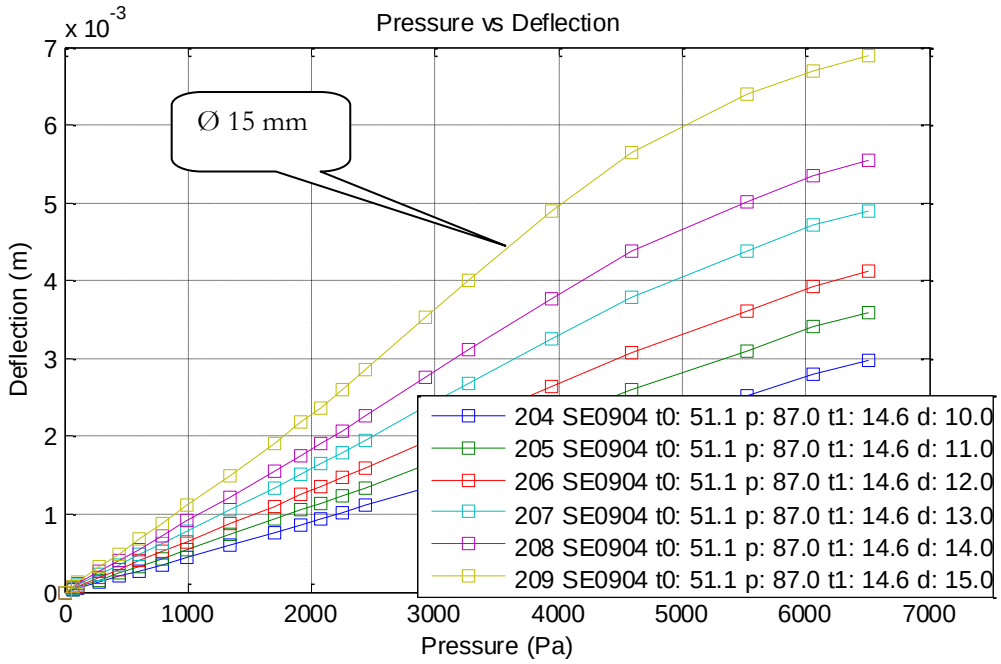

Fig. 45 Deflection versus pressure shows extreme deflection for d=15mm

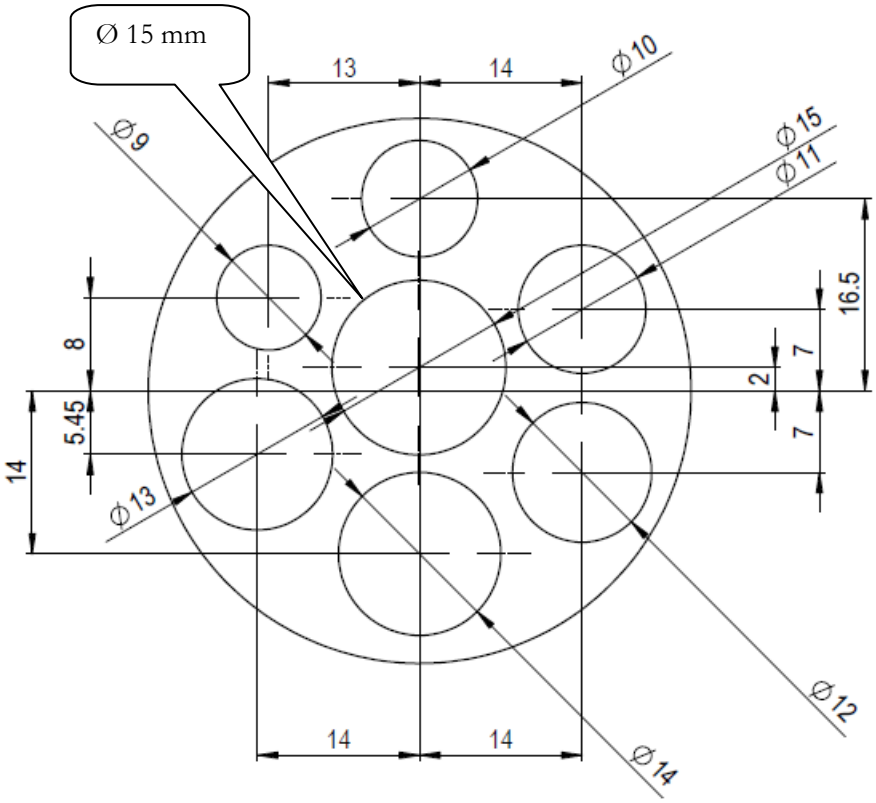

Fig. 46 Measurement tool with 15mm aperture near center

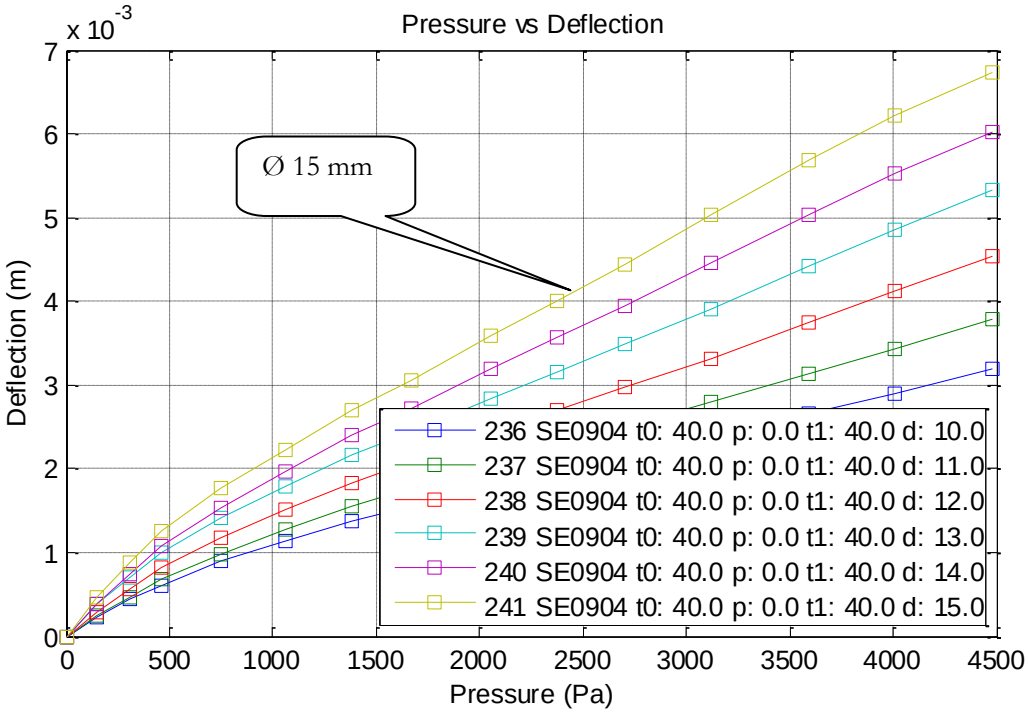

Fig. 47 Deflection versus pressure without prestrain, no extreme deflection in 15mm

4.2.13 Mooney Rivlin fit

To be able to simulate the deflection versus pressure experiments, a Mooney Rivlin hyperelastic material model is fitted to the stress strain curve. The various measurements are put together in a point cloud and are fitted by the green line. Stress calculated by using thickness/stretch in the center gave the best fitting result. Eq. 28 shows the fitted parameters used in the Mooney Rivlin equibiaxial material model (M. Wissler, 2005).

$$\sigma_{MR} = c10 * (\lambda^2 - \lambda^{-4}) - c01 * (\lambda^{-2} - \lambda^4) \quad \text{Eq. 27}$$

$$c10 = 235220$$
$$c01 = 12442 \quad \text{Eq. 28}$$

Fig. 48 Mooney Rivlin fit – thickness taken from stretch in center

4.2.14 Linear model calculations

Next to the possibility of using Mooney Rivlin's model for simulation, a linear model can be used. This model is introduced to Optotune by Dr. Rosset (Rosset, 2009). The model is based on a constant Young's modulus. This implies that the model must be an approximation. The model uses a function that compensates for the biaxial stress in the middle of the membrane. On the outsides of the membrane, the stress is much more uniaxial.

The stress has two components: an elastic contribution due to the stretching, and the eventual presence of a residual stress σ_0 , induced by the fabrication process, or by a voluntarily applied prestretch . We use the

following formula to calculate the stress in the membrane. Y^* represents the biaxial stress and can be replaced as seen in Eq. 29.

$$\sigma_{LIN} = \varepsilon_1 \alpha Y^* + \sigma_0 = \frac{Y}{1-\nu}\alpha\varepsilon_1 + \sigma_0 \quad \text{Eq. 29}$$

$$\alpha \approx (1 - 0.24\nu) \quad \text{Eq. 30}$$

$$\sigma_{LIN} = \frac{Y}{1-\nu}\left((1 - 0.24\nu)\varepsilon_1 + \varepsilon_0\right) \quad \text{Eq. 31}$$

In these formulas, *Y** is the biaxial Young's modulus, *Y* the Young's modulus, *ν* is the Poisson coefficient, and *s* is the strain. *a* is a parameter that depends on the Poisson coefficient, and which accounts for the fact that the stress state at the membrane's border is not equi-biaxial due to the clamped boundary condition. Eq. 30 is shown by Small and Nix with numerical simulations (M. Small, 1992).

Following the calculation as presented in Dr. Rosset's dissertation, the true strains needed in Eq. 31 are calculated from the engineering strains and are formulated in the following equations.

$$\varepsilon_1 = \ln(\lambda_{arc}) = \ln(l_2/l_1) \quad \text{Eq. 32}$$

$$\varepsilon_0 = \ln(\lambda_{prestrain}) \quad \text{Eq. 33}$$

Using this stress to calculate the pressure is done in the next equation. This pressure can be used when simulating a deflection versus pressure experiment, as shown in the next section. This model is presented in (Rosset, 2009).

$$p_{LIN} = \frac{2\sigma_{LIN} t_{2,area}}{R} \quad \text{Eq. 34}$$

The Young's modulus used in this linear model is Y = 0.7 MPa. Eq. 34 is the same vessel function as used before (see Eq. 2), however, the linear stress calculation and the thickness calculation are different.

4.2.15 Simulation of deflection versus pressure experiments

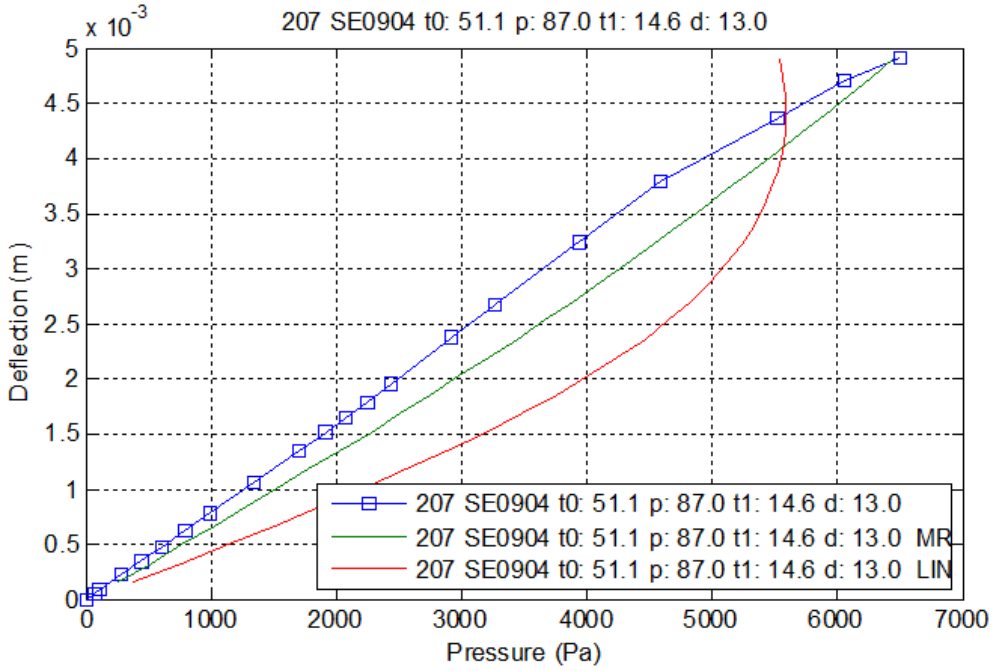

Fig. 49 One measured Deflection versus pressure curve and it's simulations (Appendix B)

In Fig. 49, two deflection versus pressure measurement results are depicted, together with Mooney Rivlin simulation curves based on the Mooney Rivlin parameters from Eq. 28. The red curve represents a simulation using a linear model based on a static Young's Modulus.

The red curve, the linear simulation, is not so far away from the measurement result. This line has been fitted by adjusting the Young's modulus as input parameter to the linear model. In all shown results (Appendix B), the Mooney Rivlin model is closer to the measurement values than the linear model. We can conclude that the Mooney Rivlin material model has a better fit.

4.2.16 Simulation error calculation

Simulations are of little value when the simulation error is not known. This section will calculate simulation errors for the Mooney Rivlin as well as the linear model. To determine the error on estimating deflection versus pressure curves, the root mean square is used.

The root mean square error method is widely used in simulation error calculation. This method is independent of error sign changes as it takes the square of the error value. Also, the calculation does not change the unit of the input values. Eq. 37 describes the calculation for a measured deflection percentage(z%) and its simulated value.

$$\epsilon_{RMS} = \sqrt{mean((z_{\%meas} - z_{\%sim})^2)} \quad \text{Eq. 35}$$

The RMS error of all measured membranes shall be evaluated, to get an indication of the error made on simulating a membrane deflection versus pressure curve. To compare various membrane diameters, the deflection has to be normalized with the radius. We then obtain a deflection percentage which can be compared through all membranes.

$$z_{\%} = \frac{z}{r} \quad \text{Eq. 36}$$

Evaluation of all measured membranes has lead to the following statistics, as shown in T. 2. Every measured membrane has its own RMS error.

Error model	RMS ($z_{\%}$)
Mooney Rivlin	0.0549
Linear model	0.1146

T. 2 Root mean squared error statistics. Mooney Rivlin's model shows the better results

The root mean square error of the Mooney Rivlin model is the lowest.

When fitting Mooney Rivlin parameters for simulating a certain membrane, it makes sense to only use closely related membranes for the fitting process. For example, if a simulation is wanted for a membrane without prestrain, the best results will be obtained when the used Mooney Rivlin parameters are fitted on experiments on membranes without prestrain.

4.3 Ring measurements

At Optotune, no research has been done before on the ring deflection next to the lens shaper (see Fig. 28). The ring deflection, depending on the pressure and membrane parameters, is an unknown. However, the shape and deflection of the ring have a large influence on the focal length of the lens when the lens is controlled open loop. There are two negative effects of a large ring deflection

- More force is needed as the ring membrane is an extra spring to be loaded
- More stroke is needed as the ring deflection takes up a large volume

A tool has been designed to measure the shape and height of the ring deflection. This tool, together with its cross section, is presented in Fig. 50. The inner radius is 3 mm. The ring starts at radius 4.2 mm and ends at radius 6 mm. The tool can be clamped in the deflection versus pressure measurement setup and then be used for experiments. Four cuts have been made to measure the ring deflection and contour from above. In the cross section, the membrane is visualized by a blue line. When pressure is applied underneath, the lens and ring will deflect upwards.

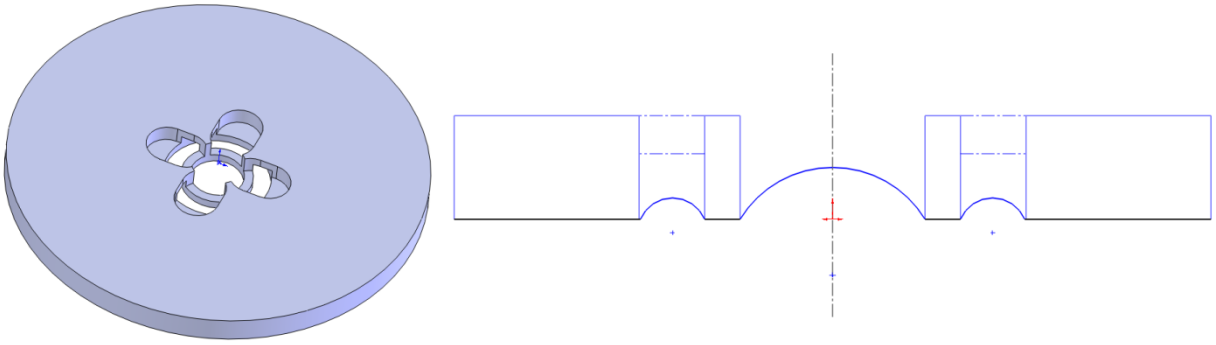

Fig. 50 Tool to create a lens and ring deflection (3d + cross section view)

4.3.1 Deflection measurements

Fig. 51 shows the result of deflection versus pressure measurements done on the ring geometry in Fig. 50. From the dark blue line and the red line, one can conclude that more prestrain on the membrane makes it stiffer. Then, from the red line to the black line, we can conclude that the thicker membrane is stiffer.

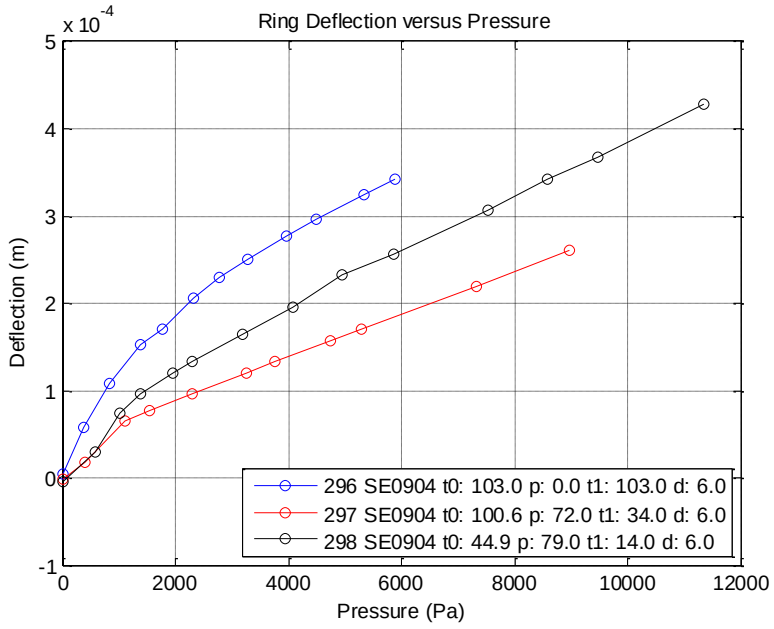

Fig. 51 Ring deflection versus pressure measurements

4.3.2 Contour measurements

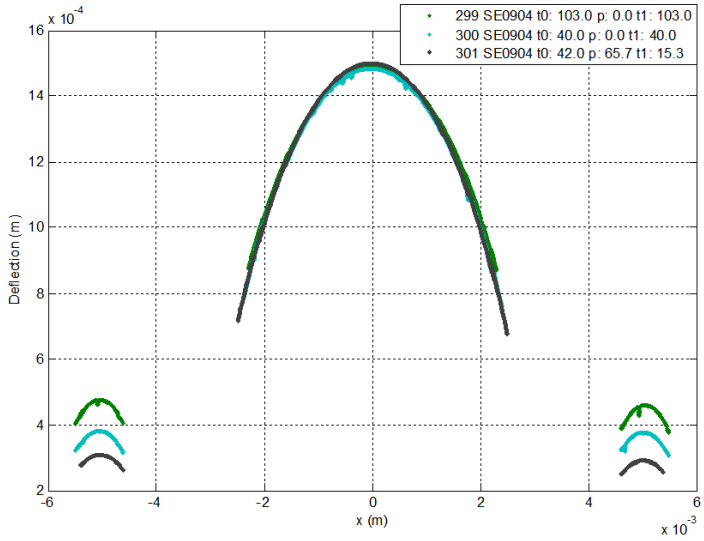

Fig. 52 Lens - Ring contour measurements

Fig. 52 shows three membranes measured with the ring deflection tool. We look at the effect of thickness and prestrain on ring deflection, at a constant lens deflection (focal length). Measurement id 300 is compared with measurement id 299, which is thicker and measurement id 301, which has more prestrain.

Increasing thickness

In Fig. 52, going from measurement id 300 to 299 by increasing thickness, one can notice the ring deflection is higher. This is possible, as the pressure is also higher (7933 Pa versus 4233 Pa) to deflect the thicker membrane lens to 1.5 mm height.

Increasing prestrain

In Fig. 52, going from measurement id 300 to 301 by increasing the prestrain, the ring deflection decreases height. The pressure increased slightly from 4233 Pa to 5240 Pa. The prestrain also caused the membrane to become thinner.

4.3.3 Calculations for a bulge ring

In this section, the stress for the ring around the lens shaper (see Fig. 28) is calculated. The complexity of the stress in the ring consists of a biaxial prestrain, combined with a uniaxial strain caused by the deflection. The same approach as to the center calculations will be used here.

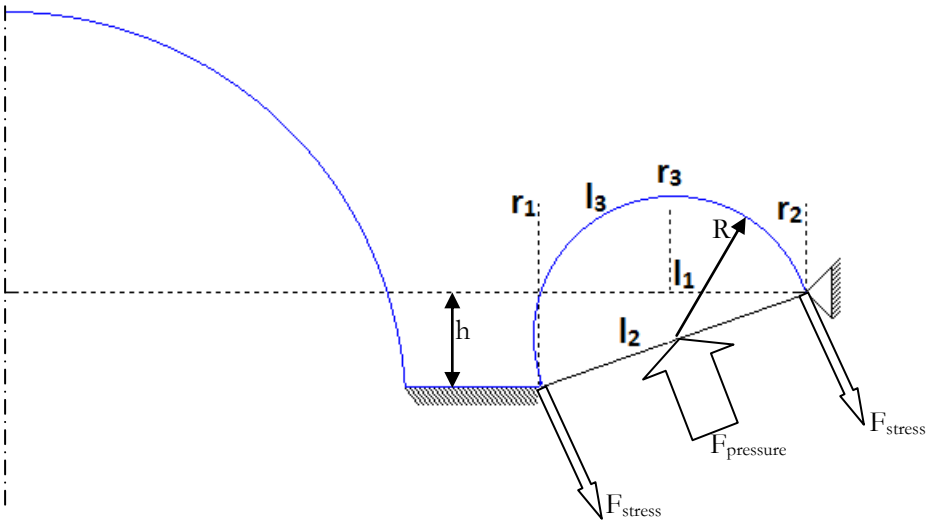

Fig. 53 F_{Stress} in the ring shaped membrane equals F_{force}

Consider a vessel under static equilibrium with a spherical surface. Newton's first law of motion states the stress around the wall must have a net resultant force that equals the internal pressure across the cross section.

$$F_{stress} = \sigma A_{wall} = \sigma 2\pi t_3 (r_3 - R + r_3 + R) \quad \text{Eq. 37}$$

$$F_{stress} = \sigma 4\pi t_3 r_3 = \sigma 2\pi t_3 (r_1 + r_2) \quad \text{Eq. 38}$$

A_{wall} exists of the circumference of r_1 and r_2.
Now to calculate the resultant force from the pressure inside the vessel. The resultant force must equal the force over the cross section, so we obtain:

$$F_{pressure} = p A_{cross} = p\, 2R \cdot 2\pi r_3 = p\, 2R\pi (r_2 + r_1) \quad \text{Eq. 39}$$

A_{cross} is modeled as the area of 2R when it travels over the circumference.

Now we can calculate the pressure in the membrane ring.

$$p = \frac{\sigma t_3}{R} \quad \text{Eq. 40}$$

$$\lambda = \frac{l_3}{l_1} \quad \text{Eq. 41}$$

$$t_3 = \frac{t_1}{\lambda} \quad \text{Eq. 42}$$

The next set of equations explains the various lengths of the membrane.

Length before prestress	l_0
horizontal projection of l_2	$l_1 = r_2 - r_1$
Rotated and stretched	$l_2 = \sqrt{(r_2 - r_1)^2 + h^2}$
Blown up	$l_3 = R\theta$

Eq. 43

4.3.4 Stress calculation - Mooney Rivlin model

As before in the center bulge section, the stress is calculated to use in deflection versus pressure simulation.

The stress calculated from the Mooney Rivlin material model exists from a uniaxial and a biaxial part. The prestrain is applied equibiaxial, whereas the stress applied when deflecting the ring is uniaxial.

$$\sigma_{MR,bi} = c10 * ({\lambda_{pre}}^2 - {\lambda_{pre}}^{-4}) - c01 * ({\lambda_{pre}}^{-2} - {\lambda_{pre}}^4) \quad \text{Eq. 44}$$

$$\sigma_{MR,uni} = \left(2 * c10 + 2 * \frac{c01}{\lambda}\right) * (\lambda^2 - \frac{1}{\lambda}) \quad \text{Eq. 45}$$

$$\sigma_{MR} = \sigma_{MR,uni} + \sigma_{MR,bi} \quad \text{Eq. 46}$$

To calculate the pressure with the Mooney Rivlin model, Eq. 40 - Eq. 42 are used. Eq. 46 describes the stress calculated by the Mooney Rivlin model.

4.3.5 Stress calculation – linear model

This section describes an adapted version of the Linear model as seen in use for the bulge center. Now this model will be applied to the ring around the lens shaper.

$$\sigma_{LIN} = Y * (\varepsilon_{pre} + \varepsilon) \quad \text{Eq. 47}$$

$$\sigma_{LIN} = Y * (\ln(\lambda_{pre}) + \ln(\lambda)) \quad \text{Eq. 48}$$

4.3.6 Simulation of ring deflection

Eq. 40 can be used in deflection versus pressure simulation. After plugging in the stress from the previous sections, the simulations are shown in this section.

In the following plots, the same Mooney Rivlin parameters and Young's modulus are used as in the deflection versus pressure simulations of the center (4.2.13).

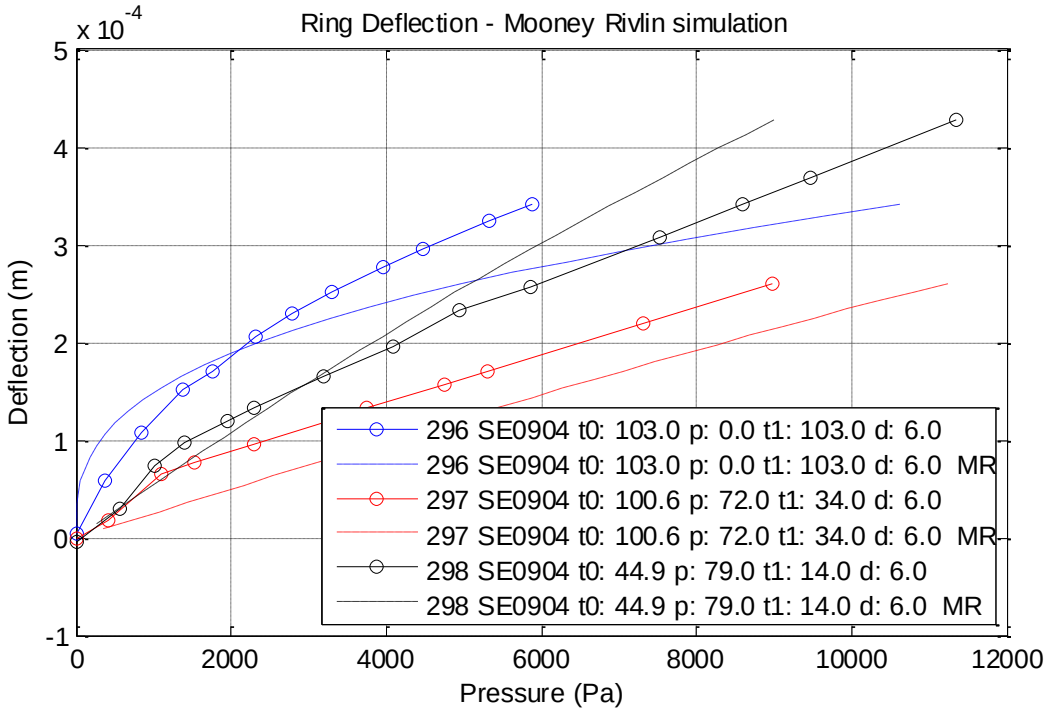

Fig. 54 Ring deflection versus pressure – Mooney Rivlin Simulation

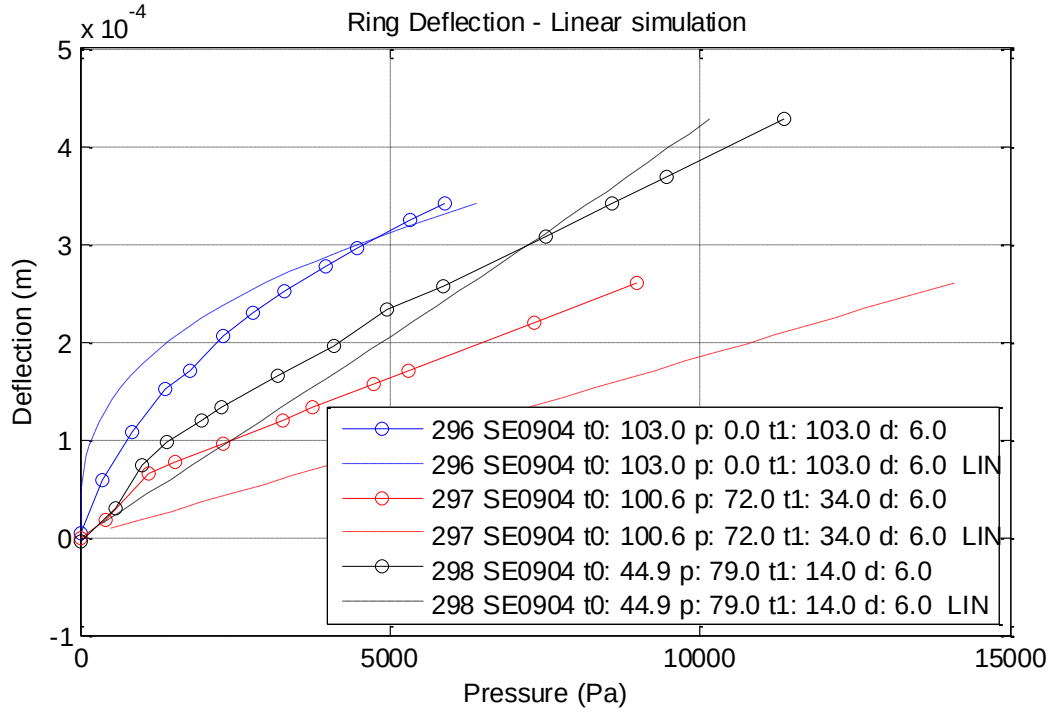

Fig. 55 Ring deflection versus pressure– Linear model Simulation

4.4 Matlab "Shape Predictor" visualization tool

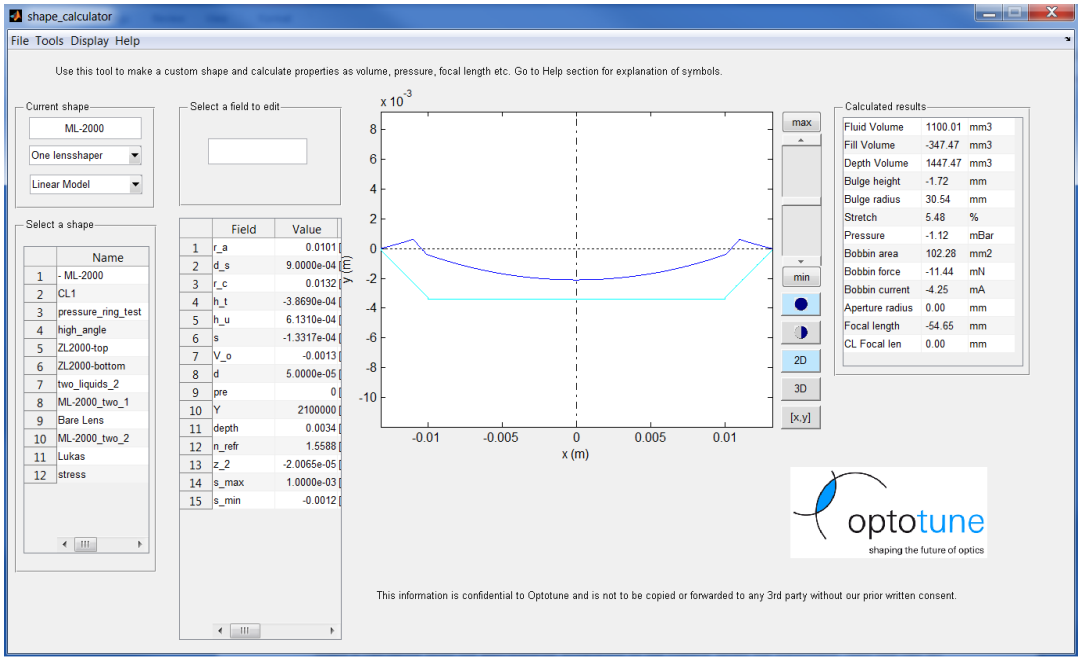

Fig. 56 Matlab tool 'Shape Predictor' shows a membrane setup according to its geometry

This interface is able to interpret geometrical values for a membrane setup and directly show the shape. The shape is calculated from the axisymmetric integration of the volume under the membrane. The pressure under the center and ring are calculated and an iteration process ensures that both pressures are the same. This means that the ring deflection and center deflection are matched in order to have a constant pressure in the fluid.

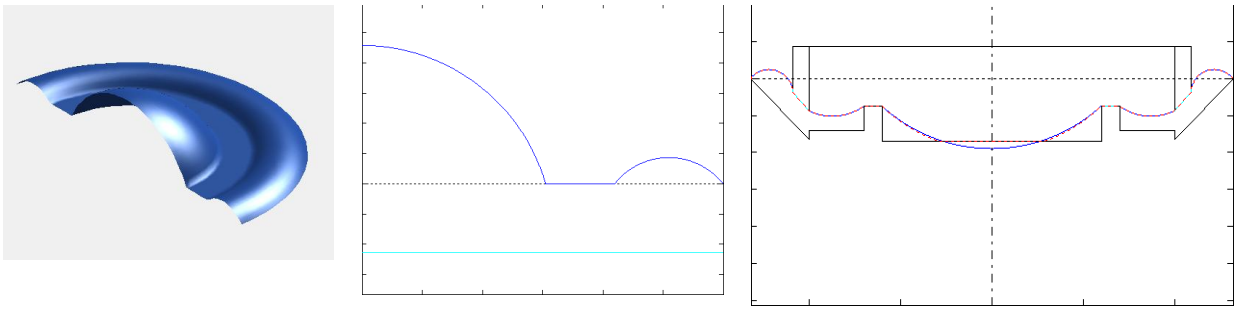

Fig. 57 Examples of simulations made in 'Shape Predictor'

Three different types of lens setups are modeled:

- no lens shaper, only a circular membrane filled with fluid
- one lens shaper to move up and down. (as in manual lens demonstrator)
- two lens shapers, one moves up and down (as in coil lens product)
- Double container, two lens shapers and two fluids

Two types of modeling are implemented:

- Linear model (Young's modulus)
- Mooney Rivlin model (c10, c01 parameters)

Furthermore, several features are implemented:

- 2D / 3D view
- Radius / Diameter view
- Aperture view
- Pressure iteration tool
- Help documentation
- Shape library
- Movie recording
- Screenshot

4.5 Membrane conclusions and outlook

The Mooney Rivlin model used by the Shapepredictor has a lower root mean square error than the previously used linear model. However, the model should be improved further and more research should be done to investigate the membrane stress-strain identification.

Conclusions

- At constant pressure, a smaller radius creates a smaller deflection. The ratio between aperture area and deflection remains constant when changing the aperture radius.
- The factor between strain over the arc length of the cross section and in the center of the bulge has been found to be approximately 0.7.
- The factor between strain over the surface area of the membrane and over the arc length of the cross section has been found approximately 0.7.
- The calculated stress strain plot based on deflection versus pressure experiments indicates that with the current production method, the membrane material model weakens when a larger prestrain is applied.
- Well fitting Mooney Rivlin parameters for the material SE0904 have been found:
  - `c10 =  232540;`
  - `c01 =  17043;`
- A well fitting Young's Modulus for the material SE0904 has been found:
  - Y = 0.7 MPa
- Various lens designs can be modeled much more accurate than before using the ShapePredictor.
- The shape of the rings between lens shaper(s) and the outside diameter has a large effect on the focal length of the lens.
- The pressure under the rings can be calculated by a developed extension of the previously used linear formula.
- Measurements can be stored in a developed measurement database

Outlook

- Deflection versus pressure measurements can be further improved by applying closed loop pressure control
- "Shapepredictor" software tool can further support rapid lens design at Optotune
- The optical shape of the membrane should be validated by inserting calculated Mooney Rivlin parameters in Finite Element Modeling software
- Membrane modeling can be improved by using a varying thickness model
- The production thickness is not constant over the membrane surface. Knowing and monitoring the thickness spread improves modeling possibilities
- The maximal stretch that the membrane experience influences the stress strain curve, according to the Mullin's effect. During production of prestrain, the maximal stretch should be monitored and used for research.
- Application of prestrain seems to induce uncertainty in stress strain plot. Identification of production sensitivity should be continued.
- Other Optotune materials can be tested according using the technique of this thesis

5 General conclusions and outlook

More detailed conclusions can be found at the end of chapter 3 and 4.

Tunable Optofluidic Aperture

Several aperture demonstrators have been developed. Although testing for various designs, fluids and materials, a dark spot caused by trapped fluid remained in the optical aperture.

The 'trapped fluid' problem has not been completely solved. All investigated solutions have unwanted disadvantages. I recommend to measure the surface shape of the aperture, when filled with a transparent fluid. An accurate measurement can validate the functionality of the tunable optofluidic aperture concept.

Membrane model identification

Deflections of axisymmetric circular membranes have been measured for varying thickness, prestrain, radius and pressure. The calculated stress versus strain curves have been used to extract a material model. A Mooney Rivlin fit to the stress strain curve improved the prediction of deflection versus pressure.

A 'ShapePredictor' tool is developed to enable Optotune employees to rapidly design a lens and calculate the amount of fluid needed, the force of the actuator etc. Furthermore, a database containing all the measurements is made.

Membrane model identification brings Optotune knowledge about their materials and production processes. This knowledge can be used e.g. to improve actuator design, material choice and production quality. The identification can be continued by:

- using the Mooney Rivlin parameters in finite element modeling and evaluating the optical surface
- evaluate the effect of prestrain production steps on stress strain behavior
- using the measured thickness profile in deflection versus pressure prediction

6 Literature

Graetzel, C. (2009). Optofluidic Lens shape (Internal report). Duebendorf.

Hongbin, Y. (2008). Optofluidic variable aperture. *Optics Letters , 33* (6), 105-110.

I. M. Ward, J. S. (2004). The Mechanical Properties of Solid Polymers. Chichester.

M. Small, W. N. (1992). Analysis of the accuracy of the bulge test in determining the mechanical properties of thin films. *Journal of Materials Research 7* , 1553-1563.

M. Wissler, E. M. (2005). Modeling of a pre-strained circular actuator made of dielectric elastomers. *Sensors and Actuators A: Physical , 120* (1), 184-192.

Müller, P. (2010). An Optofluidic Concept for a Tunable Micro-iris. *Journal of Microelectromechanical Systems , 19* (6), 1477-1484.

Rosset, S. (2009). *Metal ion implanted electrodes for dielectric elastomer actuators.* Lausanne: École polytechnique Fédérale de Lausanne (EPFL).

Appendix A Simulation action plan

1. Search in Membrane Measurement Database for earlier tests on the correct membrane material
2. If not enough measurements found, perform Deflection Pressure measurements with Pressure Tester
3. Calculate Stress Strain curve using the developed Matlab scripts
4. Fit Mooney Rivlin parameters to the stress strain curves
5. Simulate lens design with Shape Predictor software, using the fitted Mooney Rivlin parameters

Appendix B Matlab measurement database

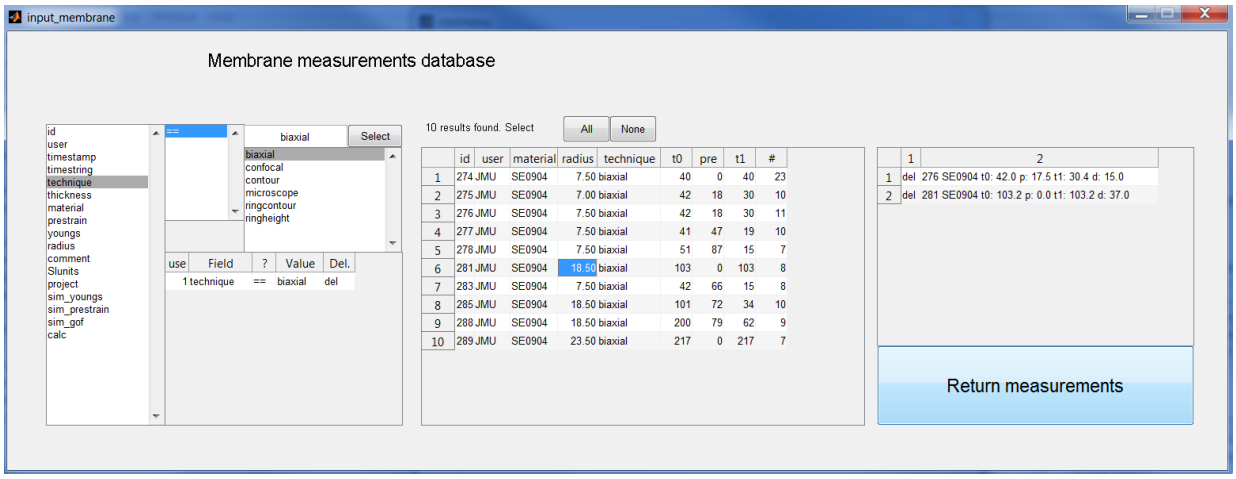

Fig. 58 Measurement database tool in MATLAB®

To save all measurements in one location, an object oriented database has been constructed. The database can be called upon as a function and returns the wanted measurements. The following code returns all measurements , having material SE0904 and measurement technique 'confocal' as an object array, without showing the guided user interface shown in Fig. 58.

```
M=input_membrane('technique','confocal','material','SE0904','showgui',0);
```

Types of measurements:

- Biaxial — Biaxial strain measurement when blowing up membrane bulge
- Confocal — Deflection versus pressure of membrane bulge
- Contour — Contour measurement of membrane surface
- Microscope — Manual microscope deflection versus pressure
- Ringcontour — Contour measurement of membrane ring surface
- Ringheight — Deflection versus pressure of membrane ring

Minimal required fields:

- User — 'JMU' , 'MAA' , 'CHG'
- Technique — 'confocal', 'biaxial'
- Timestamp — numerical time value
- Material — 'SE0904'
- Thickness — [m]
- Prestrain — [%]
- Radius — [mm]

Appendix C Matlab thesis start menu

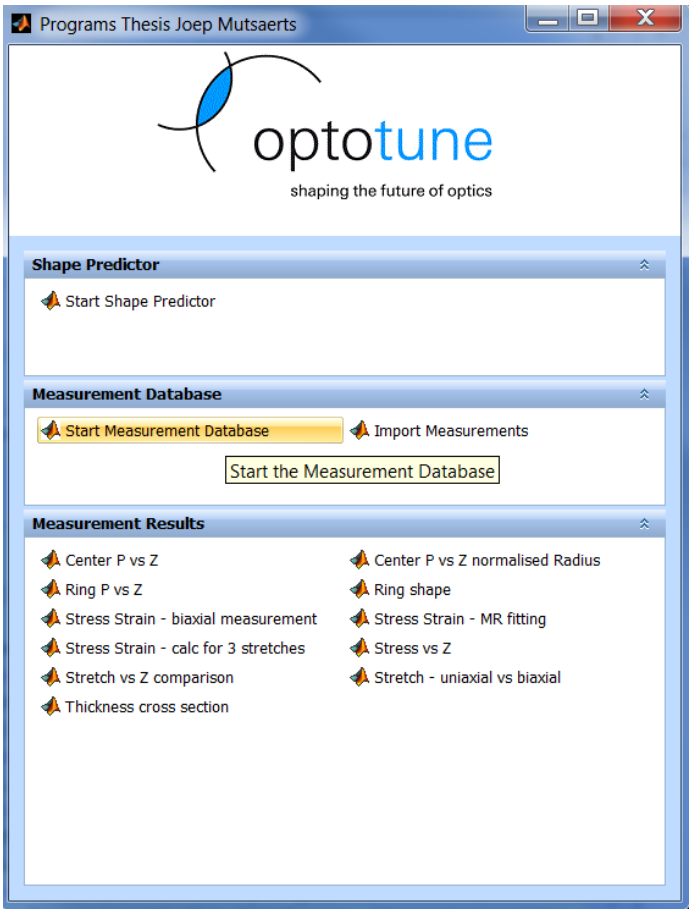

Fig. 59 Start menu displaying all Matlab work done during thesis

This Graphical User Interface is called startmenu.m and can be found in the main folder of the Matlab tools made during this thesis. Every button has a tooltip description and opens another GUI or analysis. Many of the results analysis scripts use the measurement database to select the desired measurements to use.

Appendix D Simulation plots

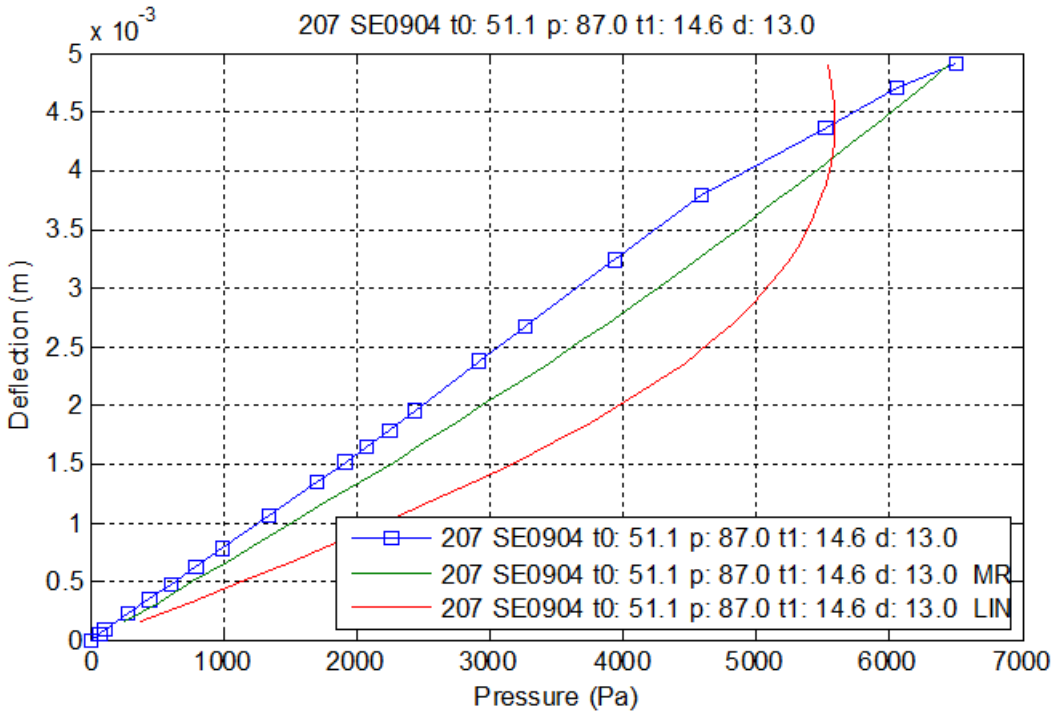

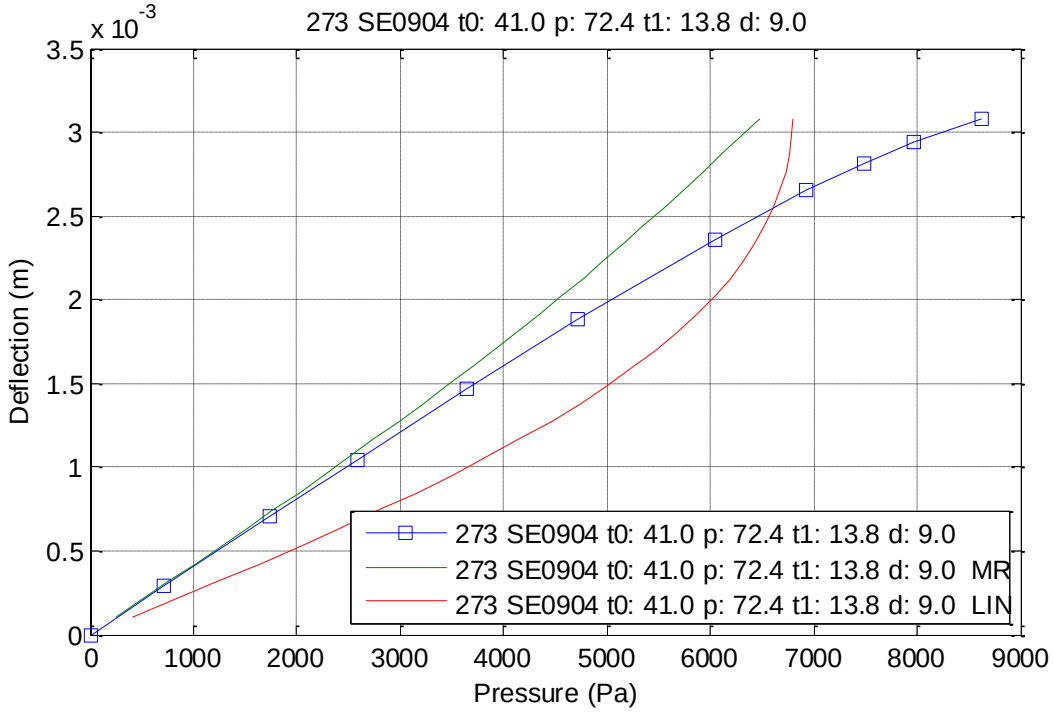

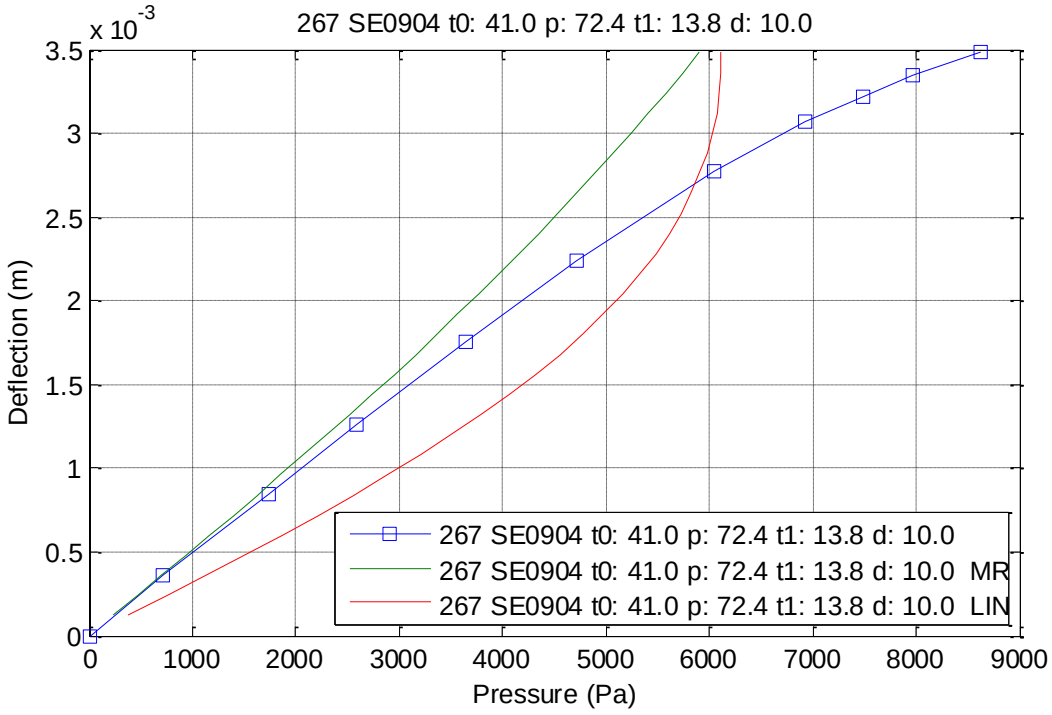
267 SE0904 t0: 41.0 p: 72.4 t1: 13.8 d: 10.0
x 10^-3
Deflection (m)
Pressure (Pa)
267 SE0904 t0: 41.0 p: 72.4 t1: 13.8 d: 10.0
267 SE0904 t0: 41.0 p: 72.4 t1: 13.8 d: 10.0 MR
267 SE0904 t0: 41.0 p: 72.4 t1: 13.8 d: 10.0 LIN

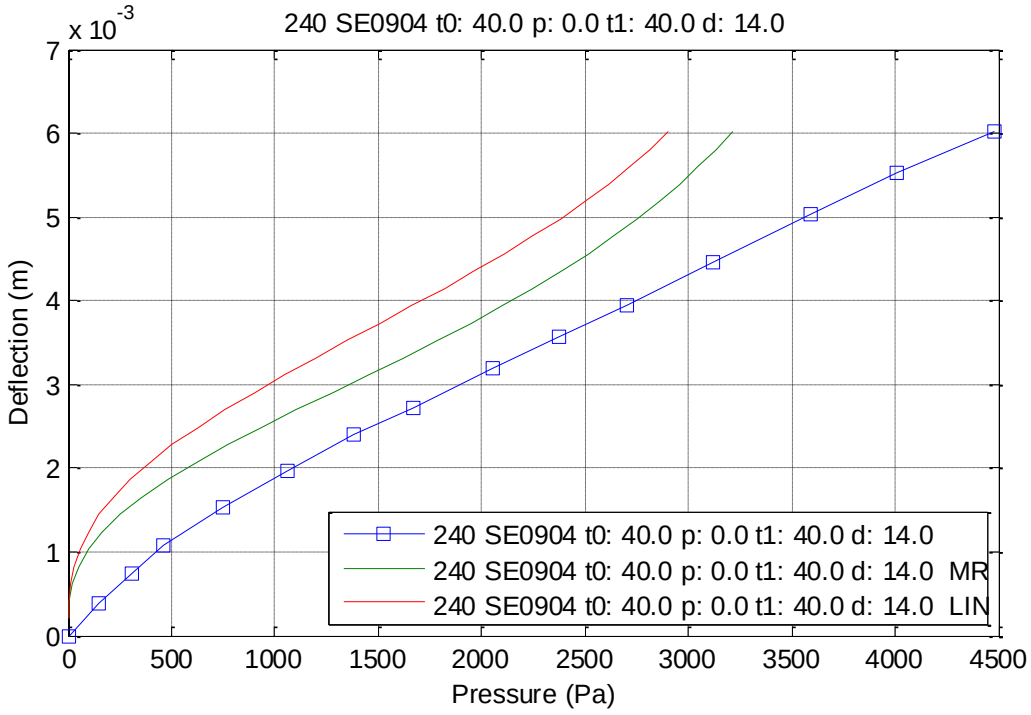
240 SE0904 t0: 40.0 p: 0.0 t1: 40.0 d: 14.0
x 10^-3
Deflection (m)
Pressure (Pa)
240 SE0904 t0: 40.0 p: 0.0 t1: 40.0 d: 14.0
240 SE0904 t0: 40.0 p: 0.0 t1: 40.0 d: 14.0 MR
240 SE0904 t0: 40.0 p: 0.0 t1: 40.0 d: 14.0 LIN

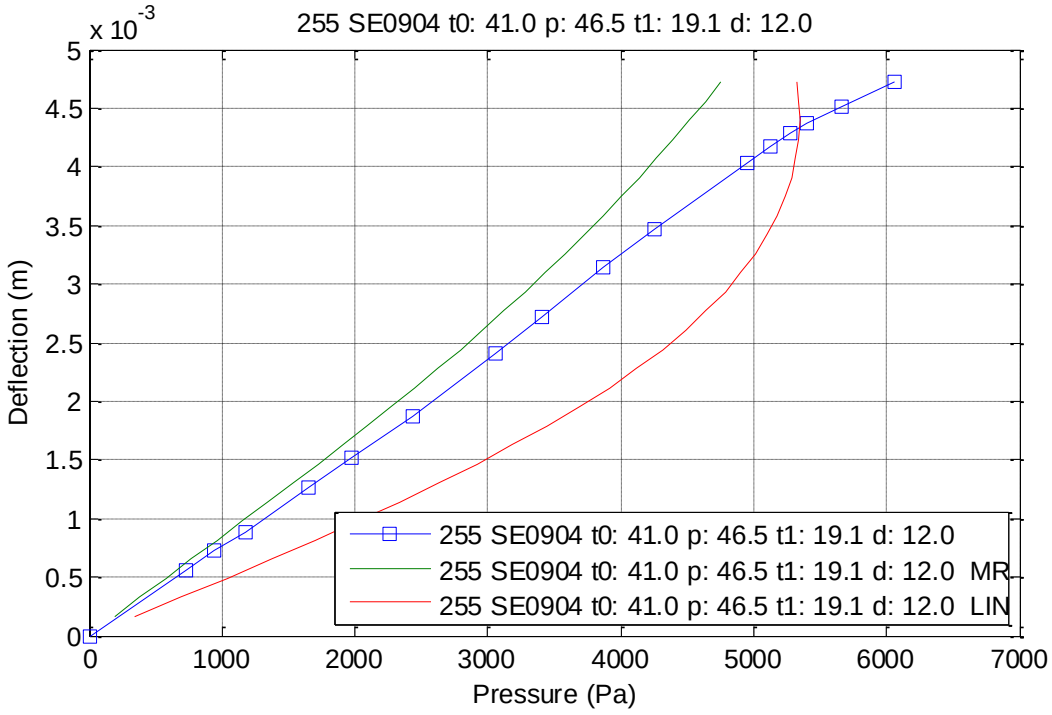
255 SE0904 t0: 41.0 p: 46.5 t1: 19.1 d: 12.0
x 10^-3
Deflection (m)
Pressure (Pa)
255 SE0904 t0: 41.0 p: 46.5 t1: 19.1 d: 12.0
255 SE0904 t0: 41.0 p: 46.5 t1: 19.1 d: 12.0 MR
255 SE0904 t0: 41.0 p: 46.5 t1: 19.1 d: 12.0 LIN

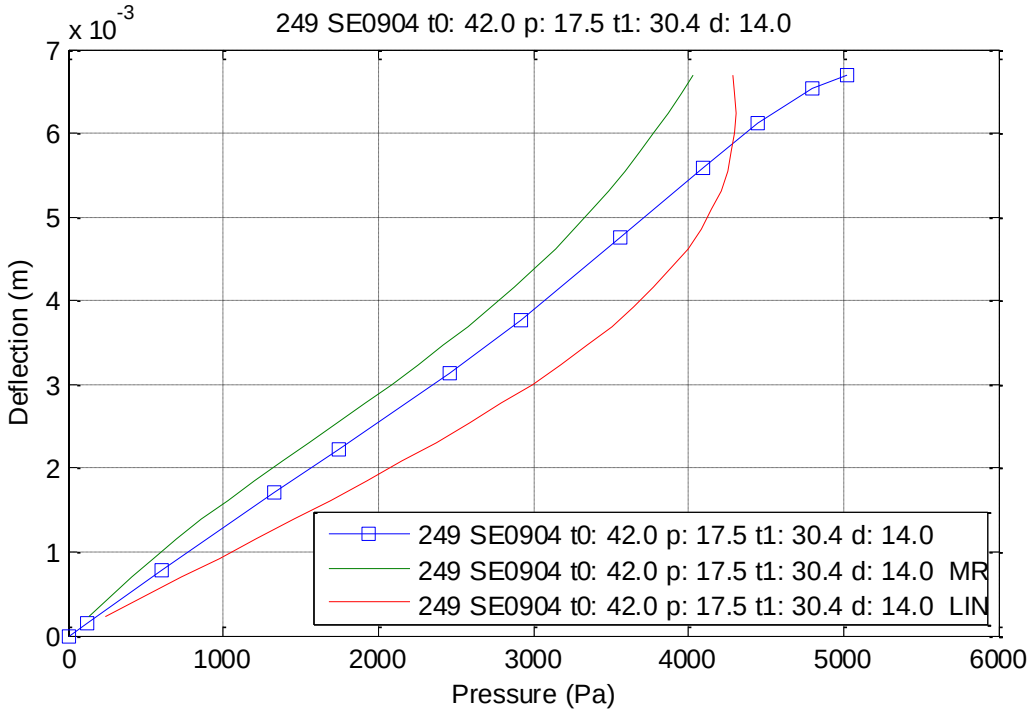
249 SE0904 t0: 42.0 p: 17.5 t1: 30.4 d: 14.0
x 10^-3
Deflection (m)
Pressure (Pa)
249 SE0904 t0: 42.0 p: 17.5 t1: 30.4 d: 14.0
249 SE0904 t0: 42.0 p: 17.5 t1: 30.4 d: 14.0 MR
249 SE0904 t0: 42.0 p: 17.5 t1: 30.4 d: 14.0 LIN

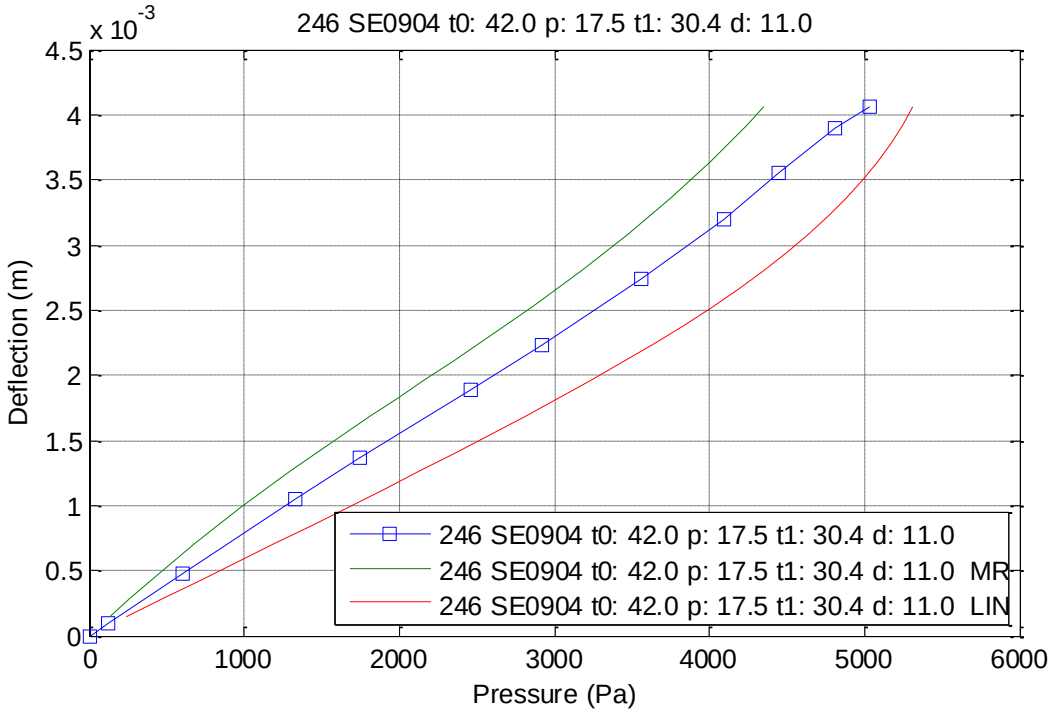
246 SE0904 t0: 42.0 p: 17.5 t1: 30.4 d: 11.0
x 10^-3
Deflection (m)
Pressure (Pa)
246 SE0904 t0: 42.0 p: 17.5 t1: 30.4 d: 11.0
246 SE0904 t0: 42.0 p: 17.5 t1: 30.4 d: 11.0 MR
246 SE0904 t0: 42.0 p: 17.5 t1: 30.4 d: 11.0 LIN

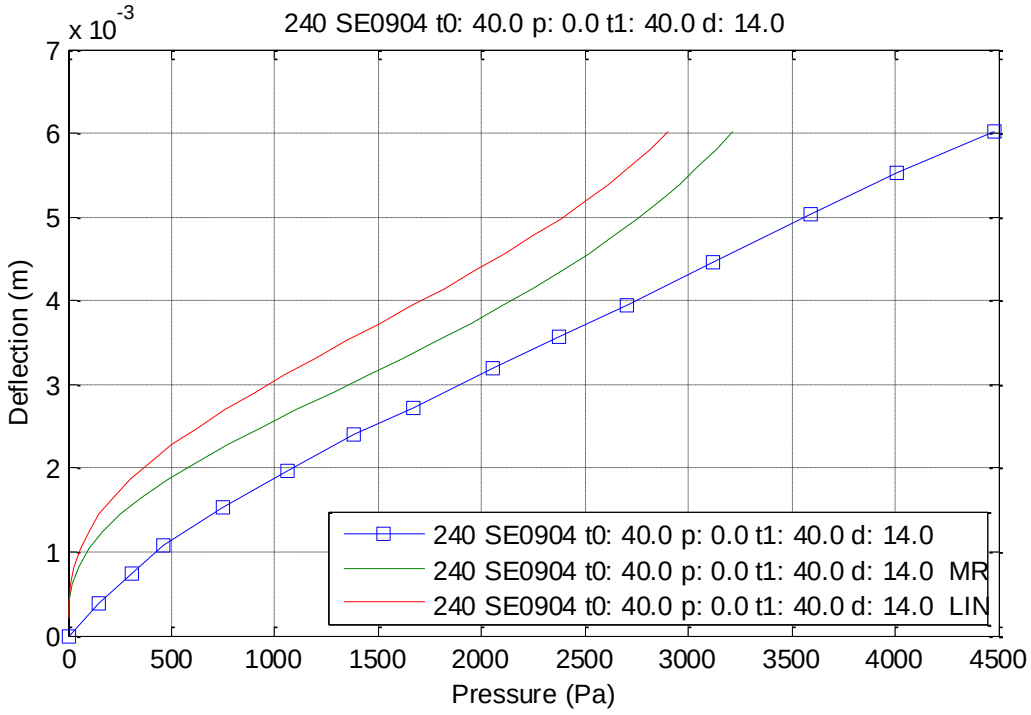
240 SE0904 t0: 40.0 p: 0.0 t1: 40.0 d: 14.0
x 10^-3
Deflection (m)
Pressure (Pa)
240 SE0904 t0: 40.0 p: 0.0 t1: 40.0 d: 14.0
240 SE0904 t0: 40.0 p: 0.0 t1: 40.0 d: 14.0 MR
240 SE0904 t0: 40.0 p: 0.0 t1: 40.0 d: 14.0 LIN